

Appendix C

Evaluation of Seismic Hazards

This Page Intentionally Left Blank

REPORT

**EVALUATION OF SEISMIC HAZARDS AT PROPOSED VANCOUVER
ENERGY OIL EXPORT TERMINAL, PORT OF VANCOUVER,
WASHINGTON**

Submitted to

**Cardno
801 2nd Avenue, Suite 700
Seattle, Washington 98104**

Prepared by

**AECOM
1501 4th Avenue, Suite 1400
Seattle, Washington 98101**

**URS Job No.: 33765022
AECOM Job No.: 60392591**

**June 8, 2015 (Rev 0)
June 24, 2015 (Rev 1)
August 7, 2015 (Rev 2)**



August 7, 2015

Alison Uno
Cardno
801 2nd Avenue, Suite 700
Seattle, Washington 98104

Report
Evaluation of Seismic Hazards at
Proposed Vancouver Energy Oil Export
Terminal, Port of Vancouver,
Washington.
URS Job No.: 33765022
AECOM Job No.: 60392591

Dear Alison:

AECOM submits Revision 2 of the subject report. Revision 1 was based on Cardno's comments of our June 8, 2015, draft, and Revision 2 was minor editing that AECOM made. Please contact us if you have additional comments.

Sincerely,

AECOM

C.B. Crouse, PhD, PE
Principal Engineer

Martin McCabe, PhD, PE
Senior Geotechnical Engineer

Mark Molinari, PG, LEG
Principal Geologist

TABLE OF CONTENTS

Contents

ACRONYMS AND ABBREVIATIONS	iii
GLOSSARY OF TERMS	iv
SUMMARY OF KEY FINDINGS	s-i
1 INTRODUCTION	1-1
2 GEOLOGIC AND TECTONIC SETTING	2-1
2.1 Cascadia Subduction Zone	2-2
2.2 Shallow Crustal Faults	2-2
2.3 Volcanoes	2-3
3 HISTORICAL AND PREHISTORIC PACIFIC NORTHWEST EARTHQUAKES	3-1
3.1 HISTORICAL EARTHQUAKES	3-1
3.2 SIGNIFICANT PREHISTORIC EARTHQUAKES	3-2
4 GROUND MOTION HAZARD	4-1
4.1 EARTHQUAKE SOURCES	4-1
4.1.1 Interplate Cascadia Subduction Zone	4-1
4.1.2 Intraplate Cascadia Subduction Zone	4-2
4.1.3 Shallow Crustal Faults	4-2
4.1.4 Random Shallow Crustal Earthquakes	4-3
4.1.5 Volcanic earthquakes	4-3
4.2 EARTHQUAKE GROUND MOTIONS	4-3
4.2.1 Ground Motions at TSVEDT Site	4-3
4.2.2 Ground Motions along BNSF Corridor in Washington	4-5
4.3 GROUND MOTIONS FOR LIQUEFACTION AND STABILITY ANALYSES	4-6
5 GROUND FAILURE HAZARDS	5-1
5.1 POTENTIAL FOR LIQUEFACTION-INDUCED GROUND DEFORMATION OR FAILURE	5-1
5.1.1 On-Shore - Areas 300 Tanks and 500 Pipeline	5-1



5.1.2	Area 400 Marine Terminal (Dock and Adjacent Transfer Pipeline)	5-2
5.2	REVIEW OF PROPOSED MITIGATION DESIGN FOR GROUND DEFORMATION/FAILURES	5-4
5.2.1	Area 300 Tanks and Area 500 Pipeline	5-4
5.2.2	Area 400 Marine Terminal.....	5-5
6	TSUNAMI AND SEICHE HAZARDS	6-1
7	SEISMIC DESIGN CONSIDERATIONS	7-1
7.1	Design for Ground Motion.....	7-1
7.1.1	Above Ground Structures	7-1
7.1.2	Buried Pipelines	7-2
7.2	Design for Permanent Ground Deformation	7-2
8	CONCLUSIONS.....	8-1
9	REFERENCES	9-1

APPENDIX – Plots of Liquefaction Potential



ACRONYMS AND ABBREVIATIONS

ASCE	American Society of Civil Engineers
BNSF	Burlington Northern Santa Fe (Railroad)
CPT	Cone Penetrometer Test
CSZ	Cascadia subduction zone
DE	Design Earthquake (per Sect. 11.4, ASCE 7-05 and ASCE 7-10 standards)
DSM	Deep soil mix
EIS	Environmental Impact Statement
g	Acceleration due to gravity ($1g = 32.2 \text{ feet/sec}^2$)
GPS	Global Positioning System
HBI	Hayward Baker Inc.
IBC	International Building Code
m.y.	Million years
M	Magnitude of earthquake
M_w	Moment magnitude earthquake scale
MCE	Maximum Considered Earthquake (per Sect. 11.4, ASCE 7-05 standard)
MCE_G	Maximum Considered Earthquake Geometric Mean (per Sect. 11.8.3, ASCE 7-10 standard)
MCE_R	Risk-targeted Maximum Considered Earthquake (per ASCE 7-10 standard)
N	Standard penetration resistance of soil (per ASTM D1586 standard)
NGVD	National geodetic vertical datum
PGA	Peak ground acceleration
PI	Plasticity Index of soil
PSHA	Probabilistic seismic hazard analysis
$S_a(0.2 \text{ sec})$	Response spectral acceleration at natural period, $T = 0.2 \text{ sec}$
$S_a(1.0 \text{ sec})$	Response spectral acceleration at natural period, $T = 1.0 \text{ sec}$
$S_a(2.0 \text{ sec})$	Response spectral acceleration at natural period, $T = 2.0 \text{ sec}$
Site Class C	Very dense soil or soft rock (per Sect. 20.3, ASCE 7-10 standard)
Site Class D	Stiff soil (per Sect. 20.3, ASCE 7-10 standard)
Site Class E	Soft soil (per Sect. 20.3, ASCE 7-10 standard)
Site Class F	Soils prone to failure (e.g., liquefaction), peats or highly organic clays, or high PI clays, or thick clay deposits (per Sect. 20.3, ASCE 7-10 standard)
SPT	Standard Penetration Test
T	Natural period of 1-degree-of-freedom undamped oscillator
T_L	Long period transition period (per Sect. 11.4.5, ASCE 7-10 standard)
T_r	Average return period
TSVEDT	Tesoro Savage Vancouver Energy Distribution Terminal
UBC	Uniform Building Code
USGS	U.S. Geological Survey
V_{\max}	Maximum velocity of point on ground during earthquake shaking
V_s	Shear-wave velocity of material
V_{s30}	Average shear-wave velocity in the upper 30m of material

GLOSSARY OF TERMS

Average shear-wave velocity in the upper 30 m of material (Vs30) – This parameter defines the overall shear stiffness of the upper 30 m (100 ft) of material at a site, and its value is the primary basis for classifying the material at the site as Site Class A, B, C, D, or E in the ASCE 7 standard. Vs30 is computed as 30 m divided by the time for a vertically propagating shear wave to travel from the ground surface to a depth of 30 m.

Cone Penetrometer Test (CPT) – Consists of pushing an instrumented steel cone of standard dimensions into soil at a constant rate and continuously measuring the resistance of the cone tip and its side friction (both in stress units) as the cone advances, then using standard correlations to interpret the type and properties of the soil being probed.

Deep soil mix (DSM) - Deep soil mixing is a ground improvement method in which cement is mixed with soil in-situ, using augers or paddles, to form in-place columns that increase the shear strength and reduce the compressibility and permeability of soft or loose ground. The soil mix columns can be overlapped and otherwise combined to treat large areas of soil.

Lateral spreading – As used in this report, lateral spreading is the horizontal movement of a soil mass due to liquefaction, and this movement occurs on sloping ground or toward a steep embankment, such as a river embankment.

Liquefaction – As used in this report, it is the transformation of saturated, loose to medium dense, primarily sandy deposits of soil from a solid state to a fluid-like state due to the increase in pore-water pressure induced by seismic shaking. Liquefaction results in settlement and can result in small to large permanent lateral movements of the ground.

Jet grout columns - Jet grouting is a ground modification system that uses compressed air and high pressure water jets to cut in-situ soil and mix it with cement, or replace the in-situ soil with a cement slurry, forming columns of moderate to high strength soil-cement or cement.

Maximum Considered Earthquake (MCE) – This term is associated with the most severe ground motion per Sect. 11.4.3 in the ASCE 7-05 standard. For the TSVEDT site, this ground motion has a 2% probability of being exceeded in 50 years, which corresponds to an average return period of 2475 years.

Maximum Considered Earthquake Geometric Mean (MCE_G) - This term is used in conjunction with the PGA (see definition below) per Sect. 11.8.3 in the ASCE 7-10 standard. For the TSVEDT site, this PGA has a 2% probability of being exceeded in 50 years, which corresponds to an average return period of 2475 years.

Peak ground acceleration (PGA) – The largest earthquake-induced ground acceleration at a particular location and in a given direction. Instruments called accelerographs record ground accelerations in three orthogonal (perpendicular) directions (2 horizontal & 1

vertical). For each of these three components, the PGA is the maximum absolute value of the recorded acceleration. As used in this report, PGA is the geometric mean of the two horizontal-component values of PGA, i.e., the square root of the product of the two horizontal-component PGA values. For soil liquefaction and stability assessments, this PGA is referred to as the MCE_G PGA.

Response spectral acceleration [$S_a(T)$] – As used in this report, it is the largest acceleration of a 5% damped single degree of freedom oscillator subjected to an earthquake ground motion. This parameter is used to compute the earthquake response of a structure.

Risk-targeted Maximum Considered Earthquake (MCE_R) - This term is associated with the most severe ground motion per Sect. 11.4.3 in the ASCE 7-10 standard and is determined for the horizontal direction that produces the maximum response of a 5% damped single degree of freedom oscillator. The MCE_R ground motion is based on risk of collapse. For the TSVEDT site, structures designed to this motion have a 1% probability of collapse in 50 years, but if the MCE_R ground motion occurs, the structures have a 10% probability of collapse.

Standard penetration test (SPT) resistance (N-value) of soil – The number of blows by a 140 lb. hammer falling 30 inches required to cause 12 inches of penetration of a 2-inch outside diameter by 26-inch long split spoon sampler into soil being investigated. The N values are used in estimating the density and selected engineering properties of the soil. See ASTM D1586 standard for details.

Vibroreplacement stone columns - Vibroreplacement is a ground improvement method which uses a vibrating probe to penetrate weak or loose soil to a desired depth and replace it with vibrated and compacted select gravel backfill, forming a “stone column”, while simultaneously densifying loose native soil around the stone column.



SUMMARY OF KEY FINDINGS

This section of the report presents the key findings of AECOM's independent evaluation of the (1) potential seismic hazards affecting the Tesoro Savage Vancouver Energy Distribution Terminal (TSVEDT) site, (2) the expected performance of the project site during seismic shaking, and (3) the proposed measures to mitigate the seismic hazards.

The seismic hazards at the site due to seiches and tsunamis in the Columbia River are negligible, as explained in Section 6.

The ground-motion hazard, per se, will be mitigated by designing the structures to applicable codes and standards. Design to the seismic provisions in these codes is judged to provide acceptable levels of seismic risk. However, the earthquake motions the facility will be designed to resist will likely induce ground failures that could result in unacceptable performance, unless the ground-failure hazard is mitigated through various ground-improvement methods. These ground-failure hazards, and the associated ground-improvement methods that have been currently proposed by the Applicant, are described below for each area of the facility.

Area 300 Tanks

For existing subsurface conditions, generally negligible soil liquefaction below a depth of approximately 45 feet, and less than approximately 4.5 inches of liquefaction-induced settlement in liquefaction-prone soils above 45 feet depth, are estimated as a result of the 2475-yr peak ground acceleration (PGA) from a great magnitude (M8.9) earthquake on the Cascadia Subduction Zone (CSZ). This event is estimated to produce less than 2 feet of lateral spreading of the ground at the tank locations. However, if the ground-improvement procedures reflected in the Hayward Baker Inc. (HBI) documents are implemented, no damage to tank foundations are anticipated for the 2475-yr shaking from this CSZ earthquake or from other non-CSZ regional earthquakes.

Area 400 Marine Terminal (Dock and Adjacent Transfer Pipeline)

For existing conditions, liquefaction to depths of approximately 85 feet below the ground surface and settlements of 9 to 11 inches, are estimated as a result of two-thirds (2/3) of the 2475-yr PGA from a great magnitude (M8.9) earthquake on the Cascadia Subduction Zone (CSZ). (The 2/3 factor is per the ASCE Standard 61-14 for Piers and Wharves). This event is estimated to produce 7 to 14 feet of lateral spreading at the dock location and at the proposed Transfer Pipeline location along the shoreline. Additional analysis of shoreline slope stability during this event indicates that the factor of safety is approximately 0.40, suggesting that substantial deformation of the shoreline embankments could occur.



The ground-improvement design in the HBI documents (illustrated schematically in Figure 5-6 at the end of Section 5) appears to allow some of the vibroreplacement stone columns to terminate at depths that may not fully penetrate the liquefiable soil zone unless additional confirmatory and mitigation efforts are employed during the stone-column installation process.

A second item of concern is that the combination of deep soil mix panels supported on top of jet grout columns is not a concept with a well-established performance record. Therefore, AECOM recommends that the anticipated performance be checked more thoroughly using advanced numerical methods such as FLAC (Fast Lagrangian Analysis of Continua) or PLAXIS. This type of computer analysis can provide more reasonable estimates of ground deformation that better assess the potential risk to the Transfer Pipeline system.

Lastly, the potential for sliding of the portions of shoreline embankment that are south of and downslope from the system of stone columns, deep soil mix panels and jet grout columns included in the design, is not diminished by the proposed ground improvements. Accordingly, if a ship is moored at the dock and is receiving petroleum from the Transfer Pipeline at the time the design seismic event occurs, a potential for deformation of the dock and displacement of the moored ship arises that would also represent a potential for a spill from the transfer system. The transfer system should be designed with sufficient flexibility to allow such movements without releasing petroleum. Alternatively, either the pile support system for the south end of the dock should be upgraded or an extension of ground improvement to the south end of the dock should be provided to prevent movement of the moored ship.

Area 500 Tank to Shoreline Pipe

The HBI documents describe ground improvement along the pipeline between the tanks and the shoreline as consisting of stone columns having tips ranging from “about Elevation -5 to about Elevation -16”. However AECOM notes that near the shoreline, i.e. near the south end of the pipeline in question, the subsurface data indicate that the depth to the non-liquefiable Troutdale Formation or dense portions of the overlying sand may be in the range of Elevation -33 to -51 or lower. AECOM therefore recommends that the tip elevation of stone column ground improvement along the pipeline be re-assessed.



1 INTRODUCTION

The purpose of this report is to provide (1) evaluations and potential impacts of the various seismic hazards on the design and performance of the proposed oil export terminal at the Port of Vancouver, Washington, hereafter referred to as the Tesoro Savage Vancouver Energy Distribution Terminal (TSVEDT), and (2) appraisal of options to mitigate the hazards at the site.

The main seismic hazards affecting the site include ground motion and associated ground-failure effects (settlement, lateral spreading, landslides into the Columbia River) triggered by soil liquefaction.

The likelihood of other seismic hazards (surface fault rupture, tsunami and seiche) is considered small and thus will not be discussed in detail.

Most of the hazard data and information presented in this report were extracted from available published reports, including the draft Environmental Impact Statement (EIS) for the site, papers, maps, and websites. Calculations of settlement and lateral spreading were made to support the evaluations of ground-failure effects.

Although the emphasis of this report is the seismic hazard at the TSVEDT site, a brief discussion of the ground-motion hazard along the Burlington Northern Santa Fe (BNSF) railroad corridor in Washington is also presented.

This report first presents introductory material on the geology, tectonics and historical seismicity of the site region in Sections 2 and 3. The ground motions at the site and along the railroad corridor were extracted from the US Geological Survey (USGS) web site, and provided in Section 4. Ground-failure hazards at the site due to soil liquefaction are analyzed in Section 5 followed by a brief discussion of the tsunami and seiche hazards (Section 6). Seismic design considerations for ground motion and permanent ground deformation are presented in Section 7. Conclusions on the seismic hazard and risk to the TSVEDT facility are summarized in Section 8. Full citations for the references cited in the report appear in Section 9.

The appendix presents plots of the results of the liquefaction analyses of the SPT and CPT data from the GRI (2013) geotechnical report for the site. The analyses were conducted using the software program, LiquefyPro.

2 GEOLOGIC AND TECTONIC SETTING

The seismotectonic setting of a site provides the framework in which the earthquake potential of geologic structures in a region can be identified and characterized. The geology of the site is important because of its impact on propagation of earthquake ground shaking to the ground surface and built structures. The following subsections provide descriptions of the seismotectonic and geologic setting of the site, and identified potential seismic sources.

The site region (southwestern Washington and northwestern Oregon) is situated along the western end of the North American tectonic plate from northern California to north of Vancouver Island, British Columbia. In this region, the offshore Juan de Fuca plate is being driven beneath the North American plate along the Cascadia subduction zone (CSZ) (Figure 2-1). The interface between these two plates occurs offshore on the seafloor at the Cascadia trench and dips east beneath the North American continent. The motion of the Juan de Fuca plate is oblique (relative to the North American plate) and is accommodated by underthrusting and subduction of the Juan de Fuca plate beneath the continent along the Cascadia trench. Oblique subduction at the Cascadia margin occurs at a rate of approximately 29 to 40 mm/yr (Figure 2-2). This plate motion has created a complex, seismically active convergent plate margin that includes shallow crustal faults and the volcanic arc in the Cascade Mountains of the Pacific Northwest that have been active during the Quaternary geologic time period (last ~1.6 million years).

Wells et al. (1998, 2002) modeled the area in western Oregon and Washington between the trench and volcanic arc (i.e. Cascadia forearc) as migrating northward along the coast and breaking up into large, clockwise rotating blocks (Figure 2-3). Recent global positioning system (GPS) results support the model and show that the western portion of the Pacific Northwest is rotating clockwise at up to 2.0°/million years (m.y.) (McCaffrey et al., 2007, 2013). This rate and direction of rotation have been occurring for approximately 16 m.y. based on geologic and geophysical (paleomagnetic) data (Wells and McCaffrey, 2013). Wells et al. (1998, 2002) differentiate between three tectonic blocks west of the Cascade volcanic arc based on contrasting patterns of deformation, seismicity and volcanism, and crustal structure. From south to north these are: the Sierra Nevada block in northern California, the Oregon Crustal block (Rotating Block), and the northern Washington block (Uplift and Transpression Zone; Figure 2-3). The Sierra Nevada block is moving in the N50°W direction at a rate of 11 mm/yr relative to stable North America. As it pushes northward it causes the clockwise rotation of the Oregon Block, which in turn compresses the Washington block against stable North America in southern British Columbia with little rotation (Figure 2-3).

The site is located in southwestern Washington at the boundary between the Oregon Crustal and Washington blocks (Figure 2-3). Other major tectonic elements of the plate boundary include (1)

an active accretionary wedge complex in the offshore region between the Cascadia trench and the coastline, (2) the Yakima Fold and Thrust Belt in Washington, and (3) the Basin and Range Province in Oregon situated east of the volcanic arc (Figure 2-3).

2.1 Cascadia Subduction Zone

The convergence between the Juan de Fuca and the North American tectonic plates along the CSZ offshore Oregon and Washington is the primary tectonic driving force in the Pacific Northwest and has the potential to generate great earthquakes of moment magnitude, $M_w \geq 8$ along the contact between these two plates, called the “interplate” portion of the CSZ. Smaller but deeper magnitude events within the Juan De Fuca plate are also possible; these earthquakes, which have occurred frequently in Puget Sound, are called “intraplate” CSZ events.

Geologic evidence collected onshore along the Pacific Northwest coast, from northern California to Vancouver Island, British Columbia, indicates that at least 16 interplate CSZ megathrust earthquakes of M_w 8 to 9+ have occurred during the last ~5,000 years (e.g., Atwater et al., 1995, 2005; Clague et al., 2000; Kelsey et al., 2005; Nelson et al., 2006, 2008). These great earthquakes result from the sudden slip between the upper surface of the Juan de Fuca tectonic plate and the lower surface of the North American tectonic plate.

The onshore data are supported and supplemented by the presence, distribution and ages of distinct sedimentary deposits (turbidites) offshore Oregon, Washington and British Columbia. These turbidites have been interpreted to be the results of submarine landslides triggered by interplate CSZ megathrust earthquakes (Blais-Stevens et al., 2011; Goldfinger et al., 2012, 2013; Hamilton et al., 2015). The Goldfinger et al. (2012) data indicate that M_w 8 to 9+ megathrust events on the interplate CSZ occur every several hundred years on average, with events on the southern portion of the interplate CSZ occurring approximately twice as frequent as the northern portion. The onshore and offshore paleoseismic records differ somewhat, and there is no consensus amongst the CSZ paleoseismology researchers on how the turbidite data should be interpreted with respect to the frequency and lateral extent of paleoearthquakes offshore of the Pacific Northwest coast (Atwater and Griggs., 2012; Atwater et al., 2014).

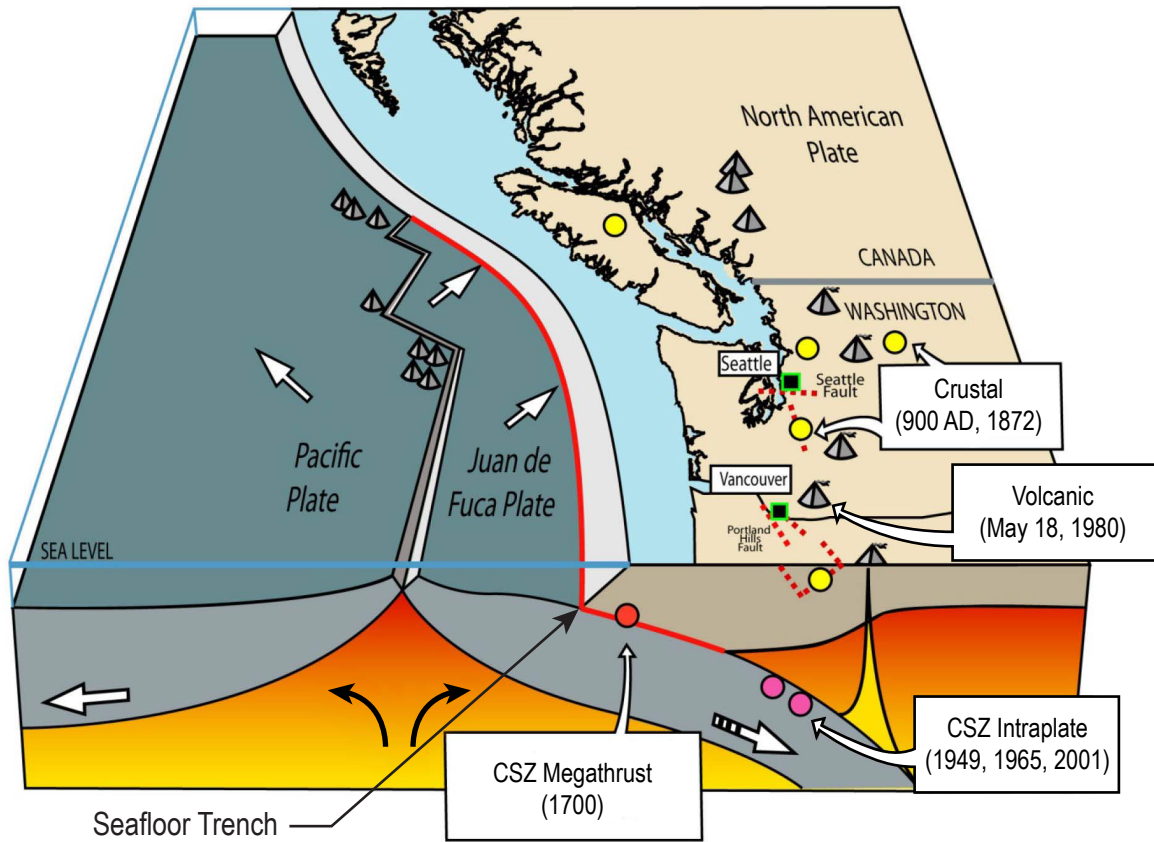
2.2 Shallow Crustal Faults

Crustal earthquakes occur during the rupture of shallow faults at depths of up to approximately 15 miles (24 km) in western Washington and Oregon. Based on Quaternary fault mapping conducted by the USGS and others in the TSVEDT site region, the East Bank Fault, Portland Hills Fault and Oatfield Fault to the southwest, and the Lacamas Lake Fault to the east (Figure 2-4), are considered to be the closest active or potentially active faults (Burns et al., 2012; Czajkowski and Bowman, 2014; Lidke et al., 2003; Mabey et al., 1993; Oregon Department of Geology and Mineral Industries (DOGAMI), 2015a; Personius et al. 2003; Phillips, 1987; USGS, 2006; Washington DGER, 2013). The mapped traces of these faults are between approximately

4 to 10 miles from the site at their closest approach. These local faults and other regional faults that exhibit evidence of Holocene (last ~10,000 years) and/or late Quaternary (last ~700,000 years) displacement or folding are considered potential sources for a shallow crustal earthquake that could cause ground shaking at the site. However, none of these faults extends through, or projects toward, the TSVEDT site. Thus, there is no potential for surface fault rupture at the site from these or other known active or potentially active regional faults.

2.3 Volcanoes

As the Juan de Fuca plate descends beneath the North American plate, it melts and generates magma (Figure 2-1) that is subsequently erupted from the chain of active volcanoes that comprise the Cascade Range, which extends roughly north-south from northern California, through Oregon and Washington to British Columbia (Figure 2-3). There have been numerous eruptions from these volcanoes in the last 4,000 years (Myers and Driedger, 2008; Figure 2-5). Mt. St Helens in southwest Washington and Mt. Hood in north central Oregon are the closest Cascade volcanoes to the site.

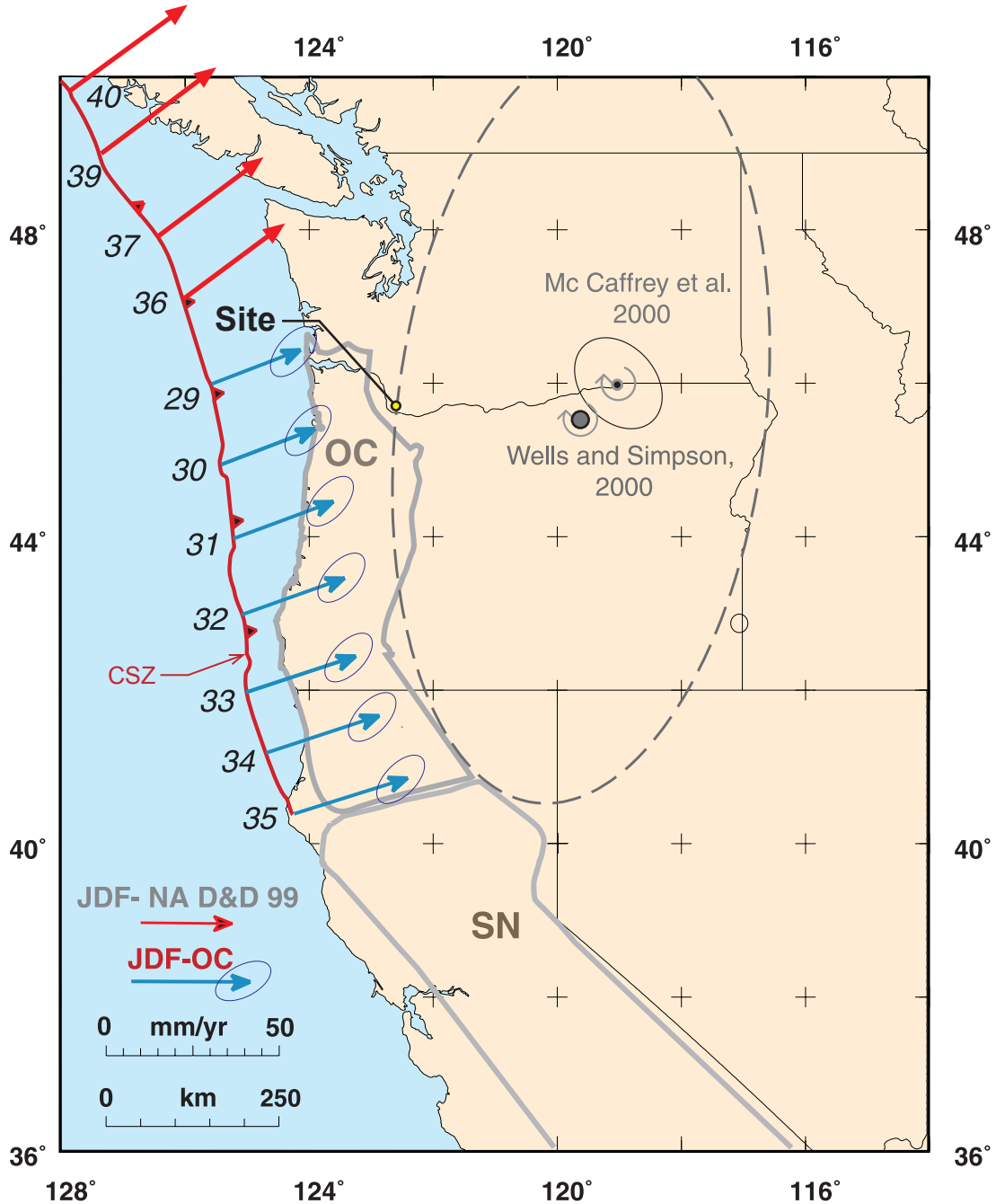


Modified from: USGS Cascadia Earthquake Sources (<http://geomaps.wr.usgs.gov/pacnw/pacnweq/casceq.html>) and Figure 3.1-2 in EFSEC TSVEDT (2013)

Legend

- CSZ Cascadia Subduction Zone
- Shallow crustal fault
- ▲ Volcano
- 1949 Year of earthquake

Figure 2-1
Tectonic Setting, Seismic Sources and Significant Earthquakes



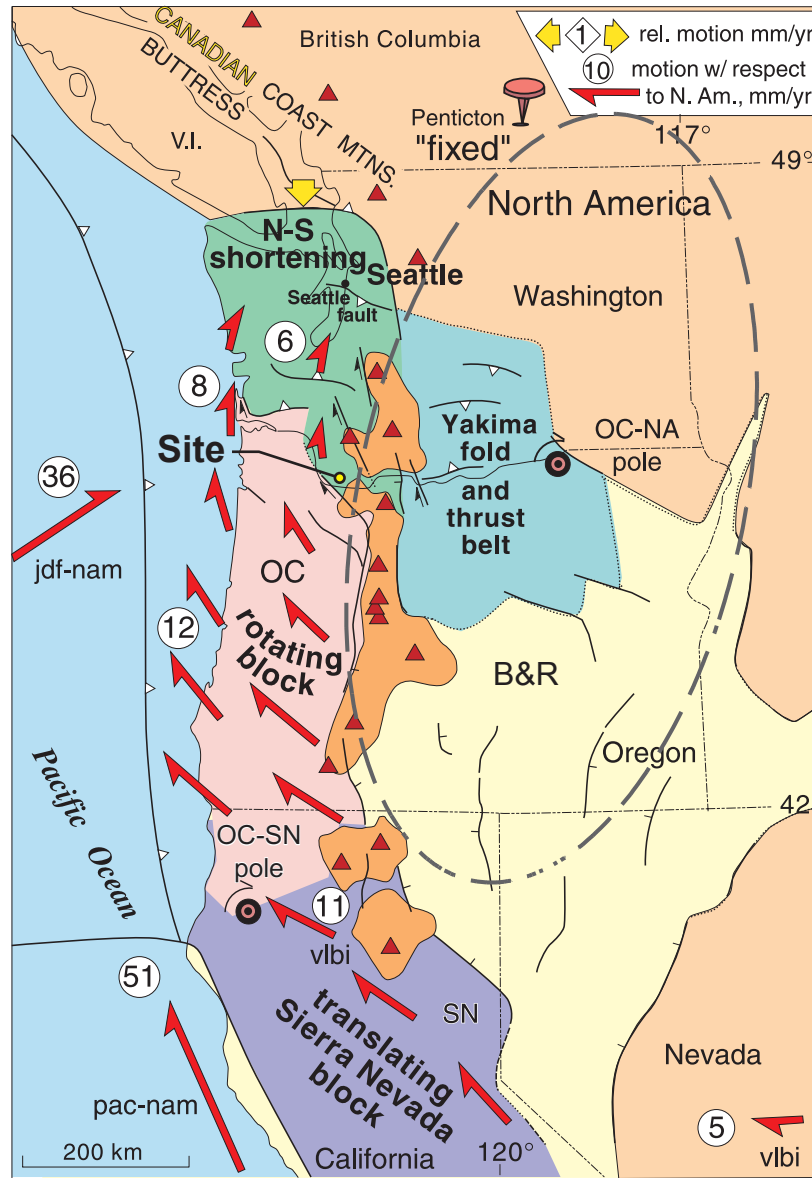
Legend

- JDF-NA Juan de Fuca – North American relative plate motion
- JDF-OC Juan de Fuca Pacific – Oregon Coastal Block relative plate motion
- CSZ Cascadia Subduction Zone Trench

Source: modified from Wells et al. (2002)

Figure 2-2

Velocity of Horizontal Convergence (mm/yr) between the Juan De Fuca Plate and North American Coast



Legend

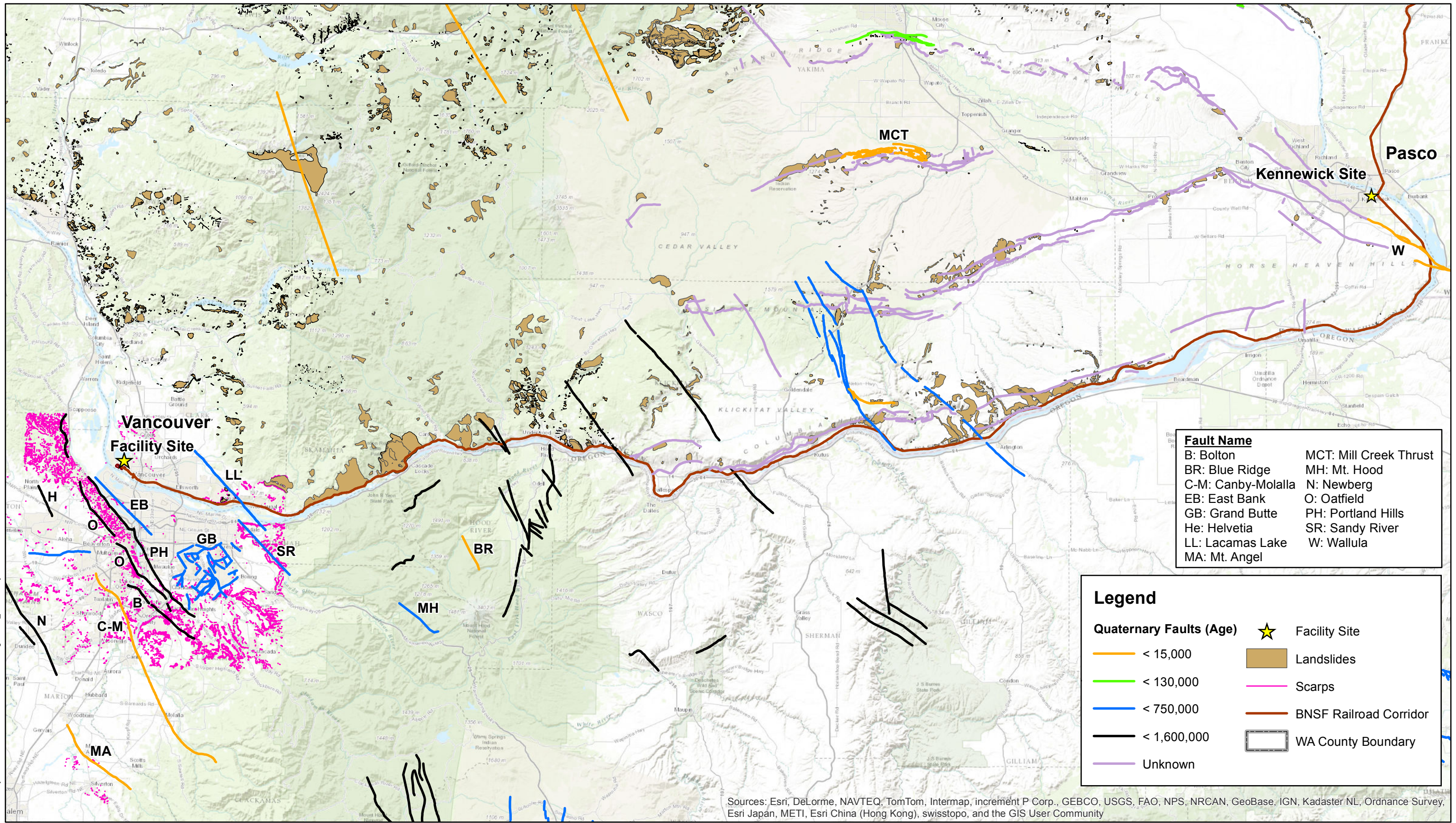
B&R	Basin & Range Province	jdf-na	Juan de Fuca –North American relative plate motion
NA	North America	pac-na	Pacific – North American relative plate motion
OC	Oregon Coastal Block		Cascade volcanic arc
SN	Sierra Nevada Block		Quaternary volcanoes
OC-NA	pole of rotation of the OC relative to North America		Relative motion direction to North America
OC-SN	pole of rotation of the OC relative to Sierra Nevada Block		Relative motion velocity in mm/yr

Source: modified from Wells et al. (2002)

Figure 2-3

Tectonic Blocks and Relative Motion to Stable North America

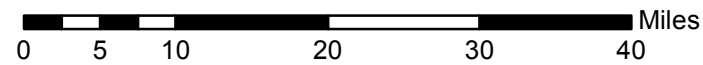
Path: J:\Projects\ICBC\Cardno-Enrtrix\GIS\MXDs\Figure 2-4_Quaternary Shallow Crustal Faults.mxd 6/18/2015



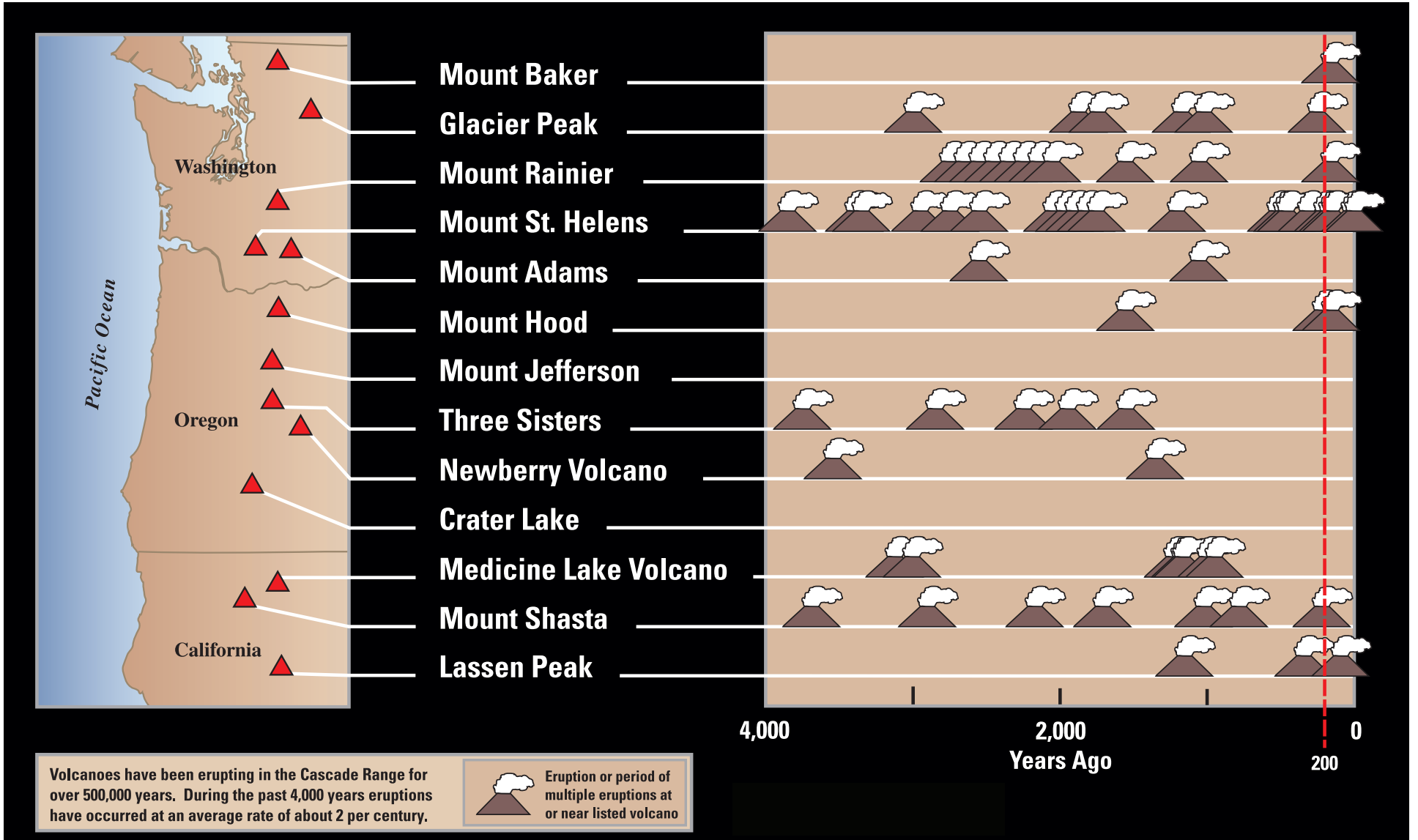
Sources: USGS; Washington Division of Geology and Earth Resources; Oregon Department of Geology and Mineral Industries

Job No. 33765022

Figure 2-4
Quaternary Shallow Crustal Faults in S. Washington and N. Oregon



Cardno EFSEC



Source: USGS (Myers and Driedger, 2008)

Figure 2-5
Volcanic Eruptions of Cascade Volcanoes
During the Past 4,000 Years

3 HISTORICAL AND PREHISTORIC PACIFIC NORTHWEST EARTHQUAKES

3.1 HISTORICAL EARTHQUAKES

The epicenters of the historical seismicity in the Pacific Northwest region are plotted on Figure 3-1 for magnitudes, $M \geq 2$; the events are coded with different symbols for magnitude and different colors for focal depth. No historical interplate CSZ megathrust earthquake of $M_w \geq 8$ has occurred, but smaller magnitude earthquakes with focal depths greater than ~20 miles have been generated by the intraplate CSZ zone within the subducted Juan de Fuca tectonic plate. Most of this seismicity is concentrated in the Puget Sound region, and this intraplate source generated the 1949 Olympia, 1965 Seattle-Tacoma (Wiest et al., 2007), and 2001 Nisqually (Ichinose et al., 2004) earthquakes of moment magnitude (M_w) 6.9, 6.7, and 6.8, respectively. Historical intraplate CSZ earthquakes near the TSVEDT site have not been recorded.

The early historical earthquakes in the Pacific Northwest date from the mid-1800s. However, the vast majority of earthquakes in Figure 3-1 occurred since 1969, the year the Pacific Northwest Seismic Network was established, which enabled the detection and accurate hypocentral locations of small magnitude events.

Volcanic seismic activity has been observed in the Mount St. Helens seismic zone since early 1980, including the M_w 5.7 eruption event on May 18. These volcanic earthquakes occurred within the Earth's crust, but most other historical crustal seismicity has not been associated with known active crustal faults.

The December 15, 1872, earthquake in the North Cascades is believed to be the largest historical earthquake in the Pacific Northwest. The exact location and magnitude of this event are uncertain; the magnitude estimates have varied between M_w 6.5 and 7.4. The felt reports place it near Chelan (Bakun et al., 2002), and a recent USGS investigation identified a surface fault rupture near southern Lake Chelan that is interpreted to be associated with the 1872 earthquake (Sherrod, 2015). The green star at 47.9°N latitude and 120.3°W longitude in Figure 3-1 is the epicenter assigned by the USGS in its 2014 seismicity database for the US. This database lists M_w 7.35 for the 1872 earthquake.

The largest historical earthquake within 20 miles of the TSVEDT site was an M_w 6.3 event on October 12, 1877. No other earthquake of $M_w \geq 6$ has occurred within this radius from the site and none has occurred within this distance from the Washington segment of the BNSF railroad corridor. The epicenter (45.5°N and 122.5°W) of the 1877 earthquake is uncertain as well as the causative fault. Three earthquakes of M_w 5.0-5.9 occurred within 20 miles of the site; the most recent event was M_w 5.3 on October 1, 1964 with an epicenter at (45.7°N and 122.8°W). It was the closest (5.5 miles) $M_w \geq 5$ event to the site.

3.2 SIGNIFICANT PREHISTORIC EARTHQUAKES

Abundant geological evidence (e.g. Atwater et al., 1995, 2005; Goldfinger et al., 2012, 2013; Nelson et al., 2006, 2008) supports the occurrence of prehistoric, great magnitude ($M_w \geq 8$) megathrust earthquakes on the interplate CSZ offshore northern Oregon and southern Washington. Information on the frequency and magnitude of these megathrust earthquakes and potential segmentation of the interplate CSZ comes from two sources: (1) records of sudden subsidence, tsunami, and liquefaction in coastal wetlands; and (2) records of submarine continental shelf and slope landslides and turbidite deposits in the deep sea off the Cascadia margin.

The most recent CSZ megathrust earthquake was on January 26, 1700. It likely ruptured the entire length of the CSZ and hence is estimated to have been $\sim M_w 9$; the date and size of this event was determined from historical tsunami records in Japan (Satake et al., 1996, 2003; Atwater et al., 2005). Using radiocarbon dating methods, Atwater and colleagues (Atwater et al., 1995, 2005; Kelsey et al., 2005; Nelson et al., 2006, 2008) have dated the occurrence of (10) other $M_w \geq 8$ events during the last $\sim 5,000$ years in western Washington and Oregon. Goldfinger et al. (2012) have documented more frequent occurrences of these size events in Oregon and Northern California based on distinct marine sediments (turbidites) interpreted to have been associated with CSZ earthquakes.

Geologic evidence for four to seven prehistoric (paleoseismic) earthquakes of $M_w \geq \sim 6.5$ in the last 3,500 years on the Seattle, Tacoma and Saddle Mountain faults in south-central Puget Sound in Washington (Figure 3-2) has been identified (Kelsey et al., 2008; Nelson et al., 2014), in addition to evidence for another large earthquake on the Seattle fault approximately 7,000 years before present (Sherrod et al., 2000). These faults are more than 100 miles from the site and therefore do not pose a hazard to the site.

Evidence of late Quaternary displacement on other faults in Washington (e.g. South Whidbey Island, Darrington-Devil's Mountain, Boulder Creek, the Utsalady Point, Lake Creek-Boundary Creek, Frigid Creek, Canyon River, Boylston Ridge, Wallula and Wenas Valley) during the Holocene has also been documented (e.g. Barnett et al., 2010, 2013; Blakely et al., 2014; Sherrod et al., 2013); however, these faults are similar to or more distant than the south-central Puget Sound faults and therefore do not pose a hazard to the site. Some, but not all of the named faults above, as well as other less well studied faults have been incorporated into the USGS seismic source model for the 2014 US national ground-motion maps. The faults in southern Washington in the USGS model are identified by name on Figure 2-4.

Late Quaternary or Holocene displacement has also been inferred or documented on several faults in northwestern Oregon (Figure 2-4); however, these faults typically have not had the more detailed investigation and age dating of paleoseismic events as the faults indicated above in Washington. However, the faults identified by name in Figure 2-4 (with the exception of the



Blur Ridge fault on Mt. Hood) are incorporated into the USGS seismic source model for the 2014 US national ground-motion maps.

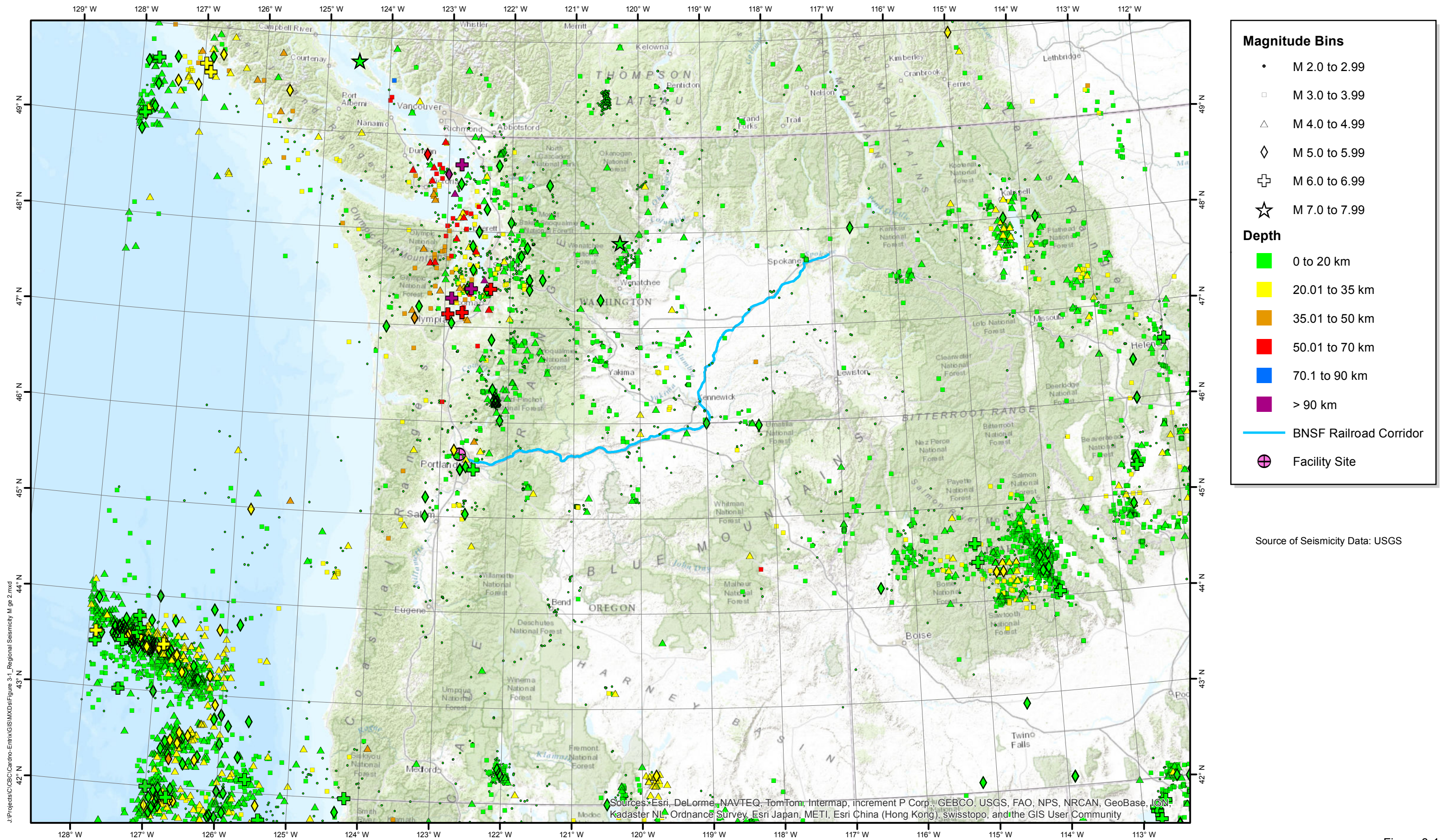
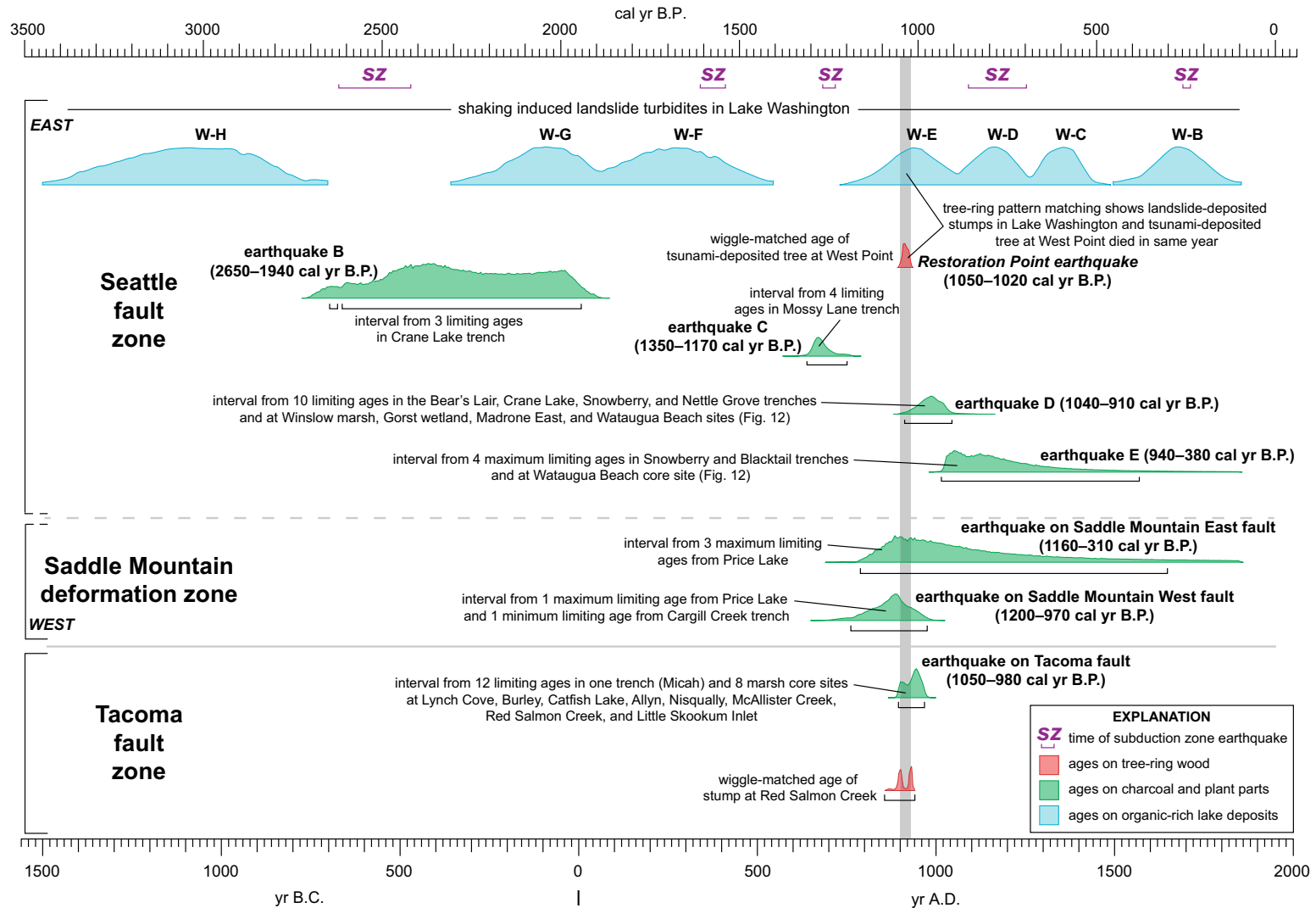


Figure 3-1

Regional Seismicity M ≥ 2



Note:

W-H = Age range for distinct Lake Washington event deposits

Source: Nelson et al, 2014

Figure 3-2
Modeled Probability of Ages of Large Earthquakes in the South-Central Puget Sound Over the Past 3,500 Years

4 GROUND MOTION HAZARD

4.1 EARTHQUAKE SOURCES

The natural sources of earthquakes capable of generating strong ground motions in the Pacific Northwest are (1) interplate CSZ, (2) intraplate CSZ, (3) shallow crustal faults, (4) randomly occurring earthquakes in the shallow crust that are not associated with known shallow crustal active faults, and (5) earthquakes of volcanic origin.

The USGS includes all five earthquake sources in its development of the US national ground-motion maps, which have been prepared during each seismic code cycle during the last ~20 years. The maps have been included in editions of the American Society of Civil Engineers (ASCE) 7 standard, beginning with the ASCE 7-98 standard published in 2000. The current 2010 edition (ASCE 7-10) is incorporated by reference in the 2012 International Building Code (IBC), which has been adopted by the State of Washington.

The USGS establishes annual earthquake recurrence rates for each of the seismic sources and also selects ground-motion prediction equations that are judged to be appropriate for computing ground motions at a site, given the occurrence of an earthquake. The USGS developed both of these inputs by soliciting inputs from regional seismic experts. Thus, the ground-motion maps and data published by the USGS are considered to be highly reliable and therefore have been used in this evaluation.

A brief discussion of the USGS modeling of these sources, and their relative contributions to the site ground-motion hazard, is presented in the following five subsections. This discussion is followed in Section 4.2 by the ground motions for the site and BNSF railroad corridor; these motions were extracted from the USGS web site, <http://earthquake.usgs.gov/hazards/>.

4.1.1 Interplate Cascadia Subduction Zone

The interplate (also called interface) CSZ is the source of great earthquakes of moment magnitude, $M_w \geq 8$, and this source is the largest contributor to the ground-motion hazard at the TSVEDT site. In its 2014 characterization of this source, US Geological Survey (USGS) included a number of possible magnitudes and rupture areas to cover the range of possible great earthquakes on the CSZ.

One scenario, called the “full CSZ rupture”, is the occurrence of megathrust CSZ earthquakes that rupture the entire interplate CSZ from Cape Mendocino, California to Vancouver Island Canada. The corresponding rupture areas, as presently modeled by the USGS (Petersen et al., 2014), are shown in Figure 4-1. The USGS considered three possible eastern extents of the rupture areas, denoted as Shallow, Preferred, and Deep, with weights of 0.2, 0.5 and 0.3, respectively; the weights represent the likelihood or probability that the fault rupture will extend to these boundaries. The USGS formally considers these eastern-extent alternatives and

associated weights in its ground-motion calculation. The western extent of the rupture in each case is the Up-dip edge (offshore deformation front), as shown in Figure 4-1.

The magnitudes of the “full CSZ rupture” scenario vary from M_w 8.6 to M_w 9.3, depending on the eastern rupture extent and the empirical magnitude/rupture-area correlation used to compute M_w . The USGS estimated these events occur once every 526 years on average (Petersen et al., 2014). The closest distances of the eastern rupture extents, the distance metric used to compute ground motion hazard at the TSVEDT site from these earthquakes, vary between 42 and 87 miles. The average recurrence interval of ($M_w \geq 8$) megathrust earthquakes north of 43.7°N was estimated to be ~350 years (Petersen et al., 2014; R. Chen, USGS, personal communication, 2015).

The other scenario the USGS considered is “partial CSZ ruptures”, i.e., earthquakes that rupture only a portion of the interplate CSZ. These events vary in magnitude from M_w 8.0 to M_w 9.1 and vary in location along the CSZ. The USGS estimated these events occur once every 711 years on average (R. Chen, USGS, personal communication, 2015).

4.1.2 Intraplate Cascadia Subduction Zone

The variable historical rate of intraplate CSZ earthquakes along the length of the CSZ, i.e., earthquakes occurring at depths greater than ~20 miles within the subducted Juan de Fuca plate, is modeled by the USGS. The largest rates are in the Puget Sound where the aforementioned M_w ~6.8 earthquakes of 1949, 1965, and 2001 occurred. Based largely on the magnitudes of intraplate subduction earthquakes elsewhere in the world, the USGS considers the intraplate CSZ as capable of generating larger events up to M 8.0; however, the rates the USGS determined for events in the magnitude interval, 7.2-8.0, were approximately once every 1,100 years on average in Western Washington and once every 6,300 years on average in Western Oregon (Petersen et al., 2014).

The site ground-motion hazard from the intraplate CSZ events is not as great as that from the $M_w \geq 8$ interplate CSZ earthquakes, primarily because of the relatively large distance (100 to 200 miles) from the site to the very active portion of this zone in the Puget Sound region.

4.1.3 Shallow Crustal Faults

Although many active faults have been identified in the Pacific Northwest, only the Portland Hills and Grant Butte faults in the immediate site vicinity have a non-negligible contribution (albeit a small one) to the 2014 USGS ground-motion hazard at the TSVEDT site. The reason for their low impact to the ground-motion hazard is due to the estimated infrequent occurrence of earthquakes on these faults and the relatively small magnitude ($M_w < \sim 7$) earthquakes these faults are considered capable of generating.

4.1.4 Random Shallow Crustal Earthquakes

The contribution to the ground-motion hazard at the TSVEDT site from random shallow crustal earthquakes varies; it is ~20 to 30% of the total ground-motion hazard for short period motions and relatively small (~few percent) for long period motions.

4.1.5 Volcanic earthquakes

Volcanic earthquakes, such as those associated with the Mt. St. Helens seismic zone, may occur in the future, but their contribution to the ground-motion hazard at the TSVEDT site is small. Mt. St. Helens is the closest volcano to the site, and it has been the most active regional volcano historically. Nonetheless, it is still relatively far from the site (45 miles) and no large historical earthquake of $M_w \geq 6$ has been recorded within its seismic zone.

4.2 EARTHQUAKE GROUND MOTIONS

The USGS has posted web-application tools that provide ground-motion data for user-specified site coordinates and soil classifications. These tools were used to gather the data for the 2008 USGS and recently released 2014 USGS national ground-motion maps, which appear in the ASCE 7-10 and in the forthcoming ASCE 7-16 standards.

4.2.1 Ground Motions at TSVEDT Site

4.2.1.1 Bedrock Motions

To prepare the ground-motion maps in the ASCE 7-10 and ASCE 7-16 standards, the USGS conducted probabilistic seismic hazard analysis (PSHA). The results (Petersen et al., 2008, 2014) reveal the TSVEDT site is in an area of moderate to high ground-motion hazard. Table 4-1 summarizes the USGS ground motions for a generic bedrock condition, which is defined as rock with an average shear-wave velocity in the upper 30 meters (V_{s30}) of 760 m/sec (2,500 ft/sec). The values listed are for the geometric mean of the two horizontal components of motion with average return periods (T_r) of 475 and 2475 years. The ground-motion parameters are peak ground acceleration (PGA) and 5% damped response spectral accelerations at natural periods of 0.2 sec and 1.0 sec, denoted as $S_a(0.2 \text{ sec})$ and $S_a(1.0 \text{ sec})$, respectively. The acceleration unit is gravity ($1g = 9.8 \text{ m/sec/sec} = 32.2 \text{ ft/sec/sec}$).

**Table 4-1
USGS Bedrock Ground Motions (g) for TSVEDT Site**

T_r - Years	2008			2014		
	PGA	$S_a(0.2 \text{ sec})$	$S_a(1.0 \text{ sec})$	PGA	$S_a(0.2 \text{ sec})$	$S_a(1.0 \text{ sec})$
475	0.191	0.435	0.151	0.167	0.369	0.128
2475	0.409	0.946	0.362	0.383	0.865	0.345

The magnitude, $M_w \geq 8$ interplate CSZ earthquakes have significant contributions to the 475-yr and 2475-yr ground motions, as indicated in Table 4-2, which lists the percentage contribution of this seismic source. These deaggregation data pertain to the 2008 USGS ground-motion values; similar data for the 2014 USGS ground-motion values are not available presently.

Table 4-2
Percentage Contribution from $M_w \geq 8$ Interplate CSZ Earthquakes to Ground-Motion Hazard at TSVEDT Site. 2008 USGS Bedrock Ground Motions.

T_r - Years	PGA	S_a(0.2 sec)	S_a(1.0 sec)	S_a(2.0 sec)
475	39	38	59	66
2475	43	41	72	82

The contributions from $M_w \geq 8$ interplate CSZ earthquakes and smaller magnitude earthquakes on other seismic sources are plotted versus magnitude and distance from the TSVEDT site in Figure 4-2 (2475-yr PGA) and Figure 4-3 (2475-yr $S_a(1.0 \text{ sec})$). The highest bar (mode) in these charts is for $M_w 9.0$ at 86.5 km (53.7 miles) on the interplate CSZ.

4.2.1.2 Ground Surface Motions

The generic bedrock condition of $V_{s30} = 760 \text{ m/sec}$ was not encountered in the geotechnical borings and CPT probes at the TSVEDT site. The borings and Cone Penetrometer Test (CPT) penetrated through layers of primarily silt and sand to a dense gravel layer, which was encountered at depths between ~60 to 100 feet beneath the ground surface. The standard penetration test (SPT), shear-wave velocity (V_s) data, and the elevation of the water table indicate the site would be classified as Site Class F, according to Chapter 20 of the ASCE 7-10 standard. This classification is due to the potentially liquefiable soils that are present. If the liquefaction hazard is mitigated through soil improvement, then those improved locations would be classified as Site Class D. Unimproved locations at the TSVEDT site would likely be classified as Site Class D or E, under the assumption that liquefaction does not occur.

Using the site coefficients in Tables 11.4-1 and 11.4-2 in the ASCE 7-10 standard, estimates of the PGA, $S_a(0.2 \text{ sec})$ and $S_a(1.0 \text{ sec})$ for Site Classes D and E were obtained by multiplying the appropriate site coefficients from these tables by bedrock accelerations in Table 4-1. The resulting accelerations are listed in Table 4-3.

**Table 4-3
Ground Motions (g) for Site Class D and Site Class E Designations at TSVEDT Site**

T _r - Years	2008						2014					
	PGA		S _a (0.2 sec)		S _a (1.0 sec)		PGA		S _a (0.2 sec)		S _a (1.0 sec)	
	D	E	D	E	D	E	D	E	D	E	D	E
475	0.271	0.338	0.631	0.830	0.332	0.506	0.245	0.328	0.556	0.782	0.294	0.439
2475	0.446	0.368	1.061	0.913	0.607	0.924	0.428	0.364	0.998	0.919	0.590	0.904

4.2.2 Ground Motions along BNSF Corridor in Washington

The ground-motion hazard diminishes along the BNSF rail corridor heading from the TSVEDT site toward the Washington-Idaho border. This corridor is shown on Figure 4-4. The points on the corridor are locations where the USGS PGA values for bedrock conditions were obtained. These values are listed in Table 4-4 and are for the geometric mean of the two horizontal components. Point No. 1 is the corridor location at the Washington-Idaho border; Point No. 28 is the last western point on the corridor before reaching the site, and Point No. 29 is just north of the site.

The geology along the corridor varies from stiff soil to Columbia River basalt (bedrock); however, geotechnical data along the route to distinguish between these two conditions were not available. The PGA values at stiff soil locations (Site Class C or D) would generally be greater than those on bedrock; in the lower ground-motion area of eastern Washington, the PGA values would be ~20 to 60% greater than the bedrock PGA values in Table 4-4. In the higher ground-motion area closer to the TSVEDT site, the amplification on stiff soil would be less (0 to ~20%).

**Table 4-4
USGS Bedrock PGA (g) for Points on BNSF Corridor**

Point No. in Figure 4-2	2008		2014	
	475-yr	2475-yr	475-yr	2475-yr
1	0.060	0.151	0.053	0.145
2	0.057	0.146	0.051	0.139
3	0.054	0.135	0.050	0.134
4	0.053	0.129	0.051	0.135
5	0.054	0.129	0.053	0.138
6	0.056	0.134	0.055	0.142
7	0.060	0.142	0.058	0.148
8	0.064	0.153	0.061	0.157
9	0.065	0.156	0.063	0.161
10	0.067	0.158	0.066	0.166
11	0.067	0.158	0.067	0.169
12	0.068	0.164	0.068	0.177
13	0.066	0.167	0.068	0.185
14	0.067	0.166	0.068	0.181
15	0.072	0.173	0.071	0.181
16	0.078	0.186	0.075	0.188
17	0.082	0.194	0.078	0.193
18	0.083	0.192	0.078	0.192
19	0.083	0.185	0.078	0.186
20	0.085	0.183	0.080	0.185
21	0.087	0.182	0.083	0.187
22	0.093	0.192	0.088	0.198
23	0.102	0.209	0.097	0.214
24	0.114	0.233	0.109	0.236
25	0.131	0.267	0.122	0.264
26	0.143	0.294	0.131	0.285
27	0.164	0.341	0.150	0.335
28	0.189	0.402	0.165	0.376
29	0.189	0.405	0.165	0.378

4.3 GROUND MOTIONS FOR LIQUEFACTION AND STABILITY ANALYSES

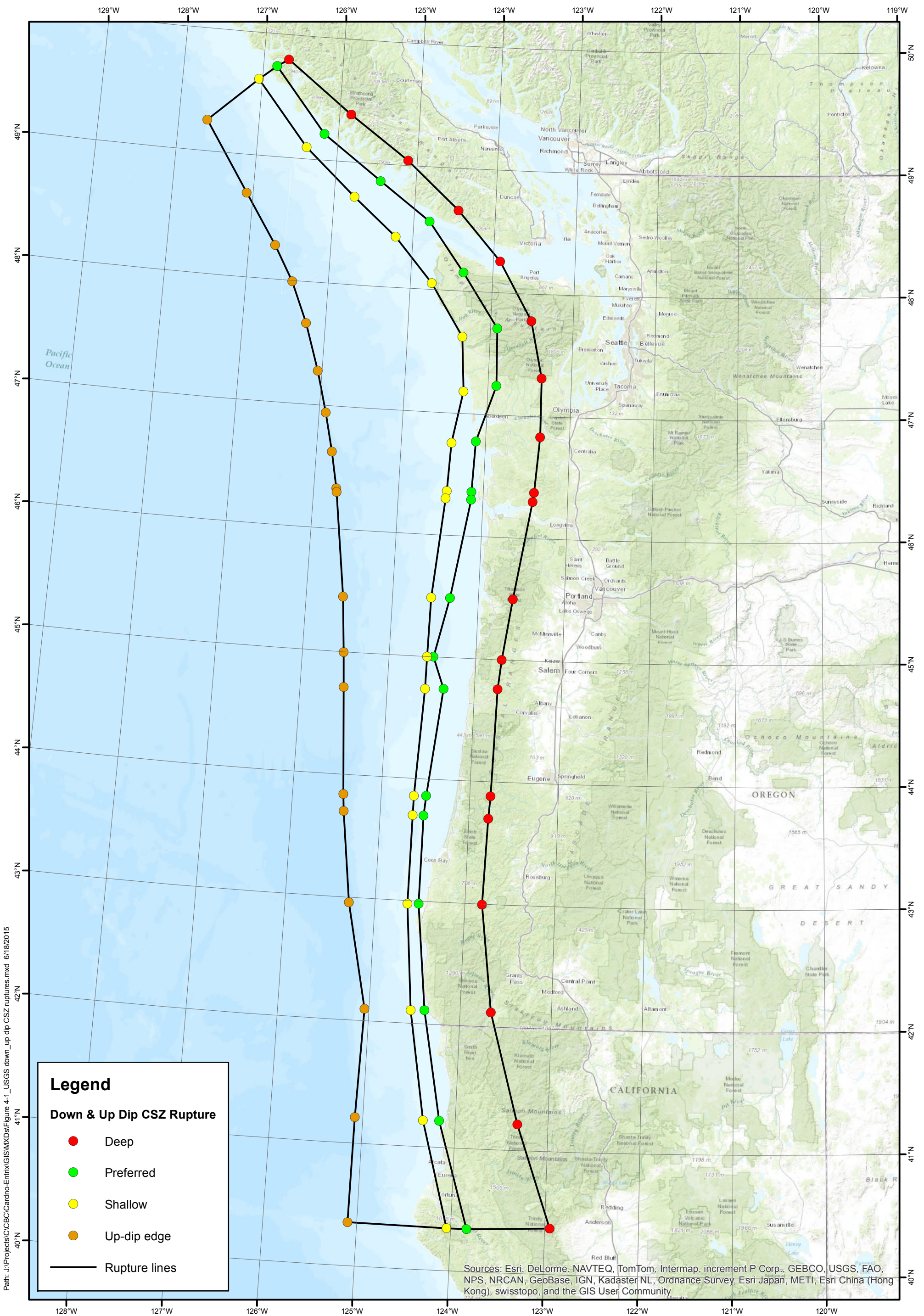
The ground-motion parameters used in the liquefaction and slope-stability evaluations in Section 5 were derived from the 2008 USGS deaggregation data. These data were used to separate the ground-motion hazard from the $M_w \geq 8$ interplate CSZ earthquakes from the smaller magnitude events on all other earthquake sources. The reason for this separation was that liquefaction also

depends on duration of shaking (not just PGA), and $M_w \geq 8$ interplate CSZ earthquakes will have much longer duration than the other types of regional earthquakes. The procedure (URS, 2011a) to derive the PGA values from the deaggregation data for these two earthquake scenarios was as follows:

- (1) Construct bedrock PGA hazard curves from the USGS 475-yr, 975-yr, 2475-yr, and 4975-yr deaggregation data for the $M_w \geq 8$ interplate CSZ earthquakes and for all other events combined. These data were obtained from the USGS interactive web site, <http://geohazards.usgs.gov/deaggint/2008/>, by entering the site coordinates.
- (2) scale these bedrock PGA by the PGA site coefficients for Site Class D in Table 11.8-1 of the ASCE 7-10 standard, and
- (3) read the 2475-yr PGA values from the two scaled hazard curves; these values are associated with the Maximum Considered Earthquake Geometric Mean (MCE_G) PGA in Section 11.8.3 of ASCE 7-10.

The resulting PGA values were 0.34g ($M_w \geq 8$ interplate CSZ earthquakes) and 0.39g (all other earthquakes). [As an aside, the total 2475-yr PGA, derived from adding both hazard curves, was 0.45g.] The associated magnitudes were computed as the mean values obtained from the 2475-yr deaggregation data and were as follows: $M_w 8.9$ (interplate CSZ earthquakes) and $M_w 6.5$ (all other earthquakes). These two PGA- M_w pairs were used to evaluate the liquefaction potential of the upland locations. At the Area 400 terminal location, the PGA values were multiplied by 2/3 to obtain the Design Earthquake (DE) ground-surface PGA for the liquefaction and slope stability assessment. The 2/3 factor converts the MCE_G PGA to DE PGA, which is required for the liquefaction assessment, per Sect. 11.8.3 of ASCE 7-05, as referenced in the ASCE 61-14 standard for the seismic design of piers and wharves, and Chapter 18 of the 2006 IBC.

The Youd et al. (2002) method was used to determine the permanent ground deformation due to lateral spreading caused by liquefaction. The same two magnitudes were used ($M_w 8.9$ - interplate CSZ earthquakes, and $M_w 6.5$ - all other earthquakes), but a distance parameter, R , defined as the horizontal distance from the site to the nearest point on the seismic source, was also required. For this application, R was computed as the mean value from the deaggregation data in the same way the mean M_w was computed. The values were 96 km (60 miles) and 30 km (19 miles).



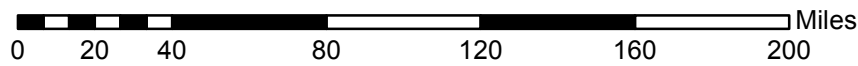
Path: J:\Projects\CBC\Cardno-Entrix\GIS\MXDs\Figure 4-1_USGS down_up dip CSZ ruptures.mxd 6/18/2015

Source of Data: R. Chen (USGS, pers. comm., 2015)

Job No. 33765022

Figure 4-1

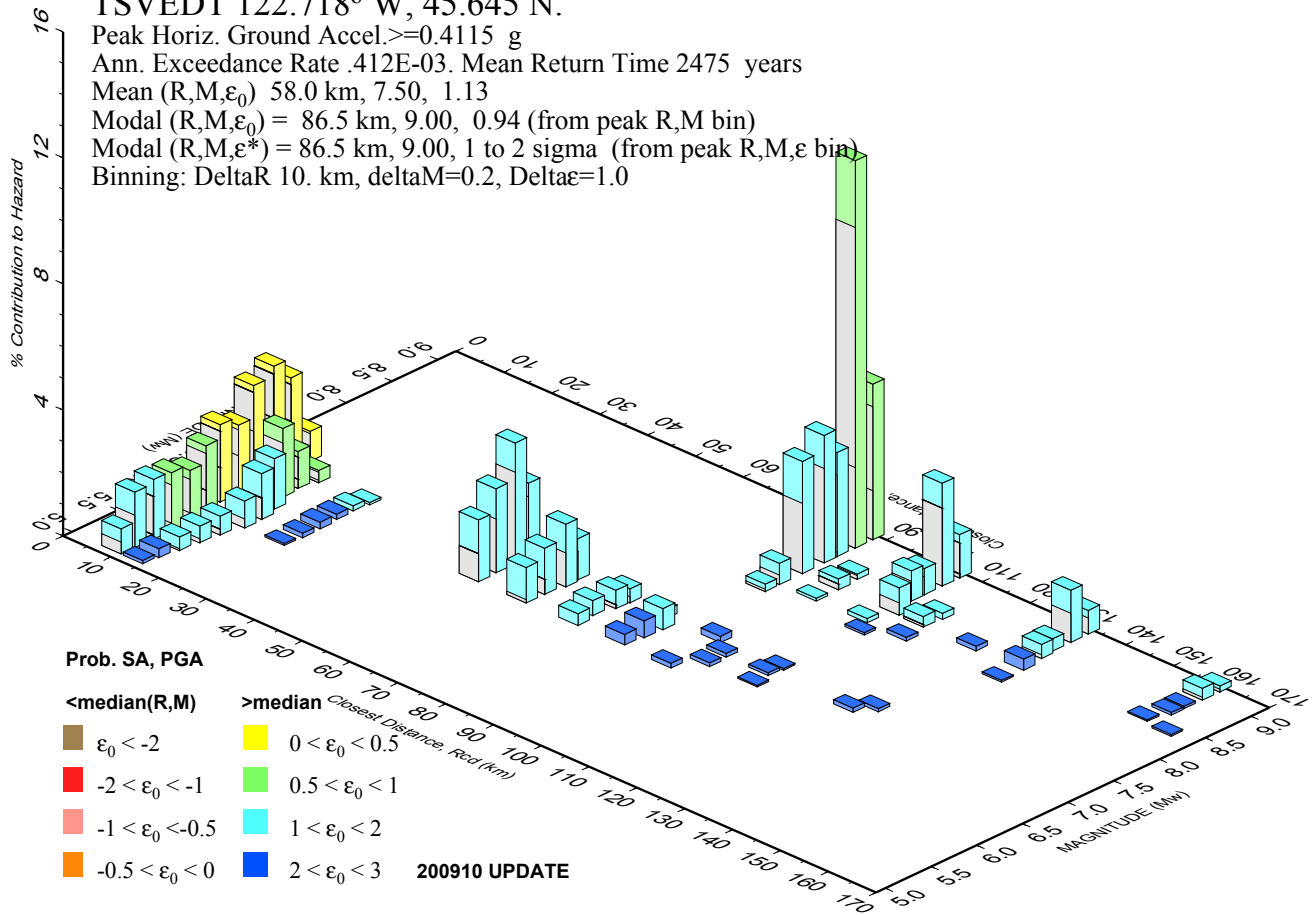
USGS Down & Up Dip CSZ Ruptures



Cardno EFSEC

**PSH Deaggregation on NEHRP BC rock
TSV EDT 122.718° W, 45.645 N.**

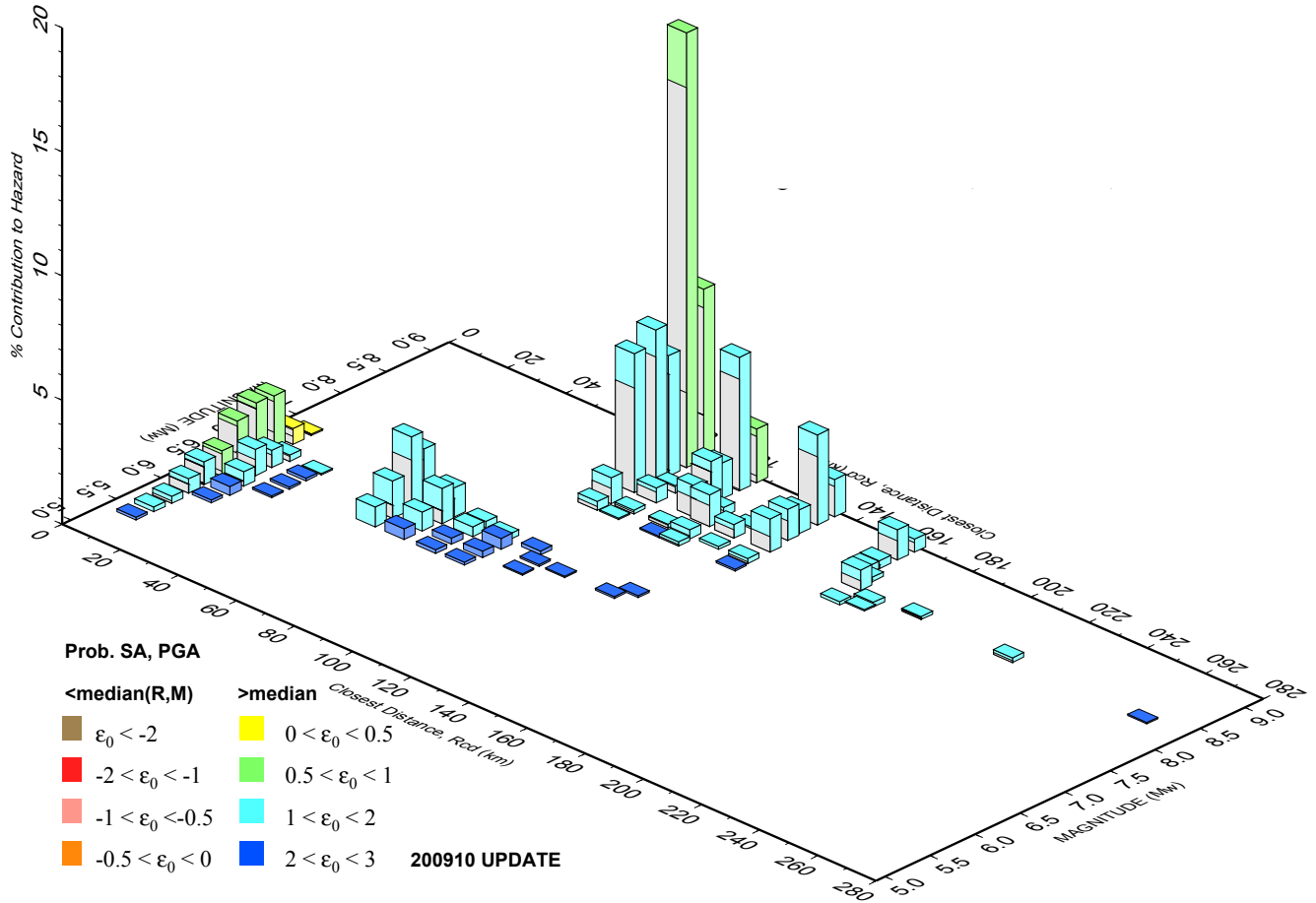
Peak Horiz. Ground Accel. ≥ 0.4115 g
 Ann. Exceedance Rate .412E-03. Mean Return Time 2475 years
 Mean (R,M, ϵ_0) 58.0 km, 7.50, 1.13
 Modal (R,M, ϵ_0) = 86.5 km, 9.00, 0.94 (from peak R,M bin)
 Modal (R,M, ϵ^*) = 86.5 km, 9.00, 1 to 2 sigma (from peak R,M, ϵ bin)
 Binning: DeltaR 10. km, deltaM=0.2, Delta ϵ =1.0



Source: USGS web site, <http://geohazards.usgs.gov/deaggint/2008/>

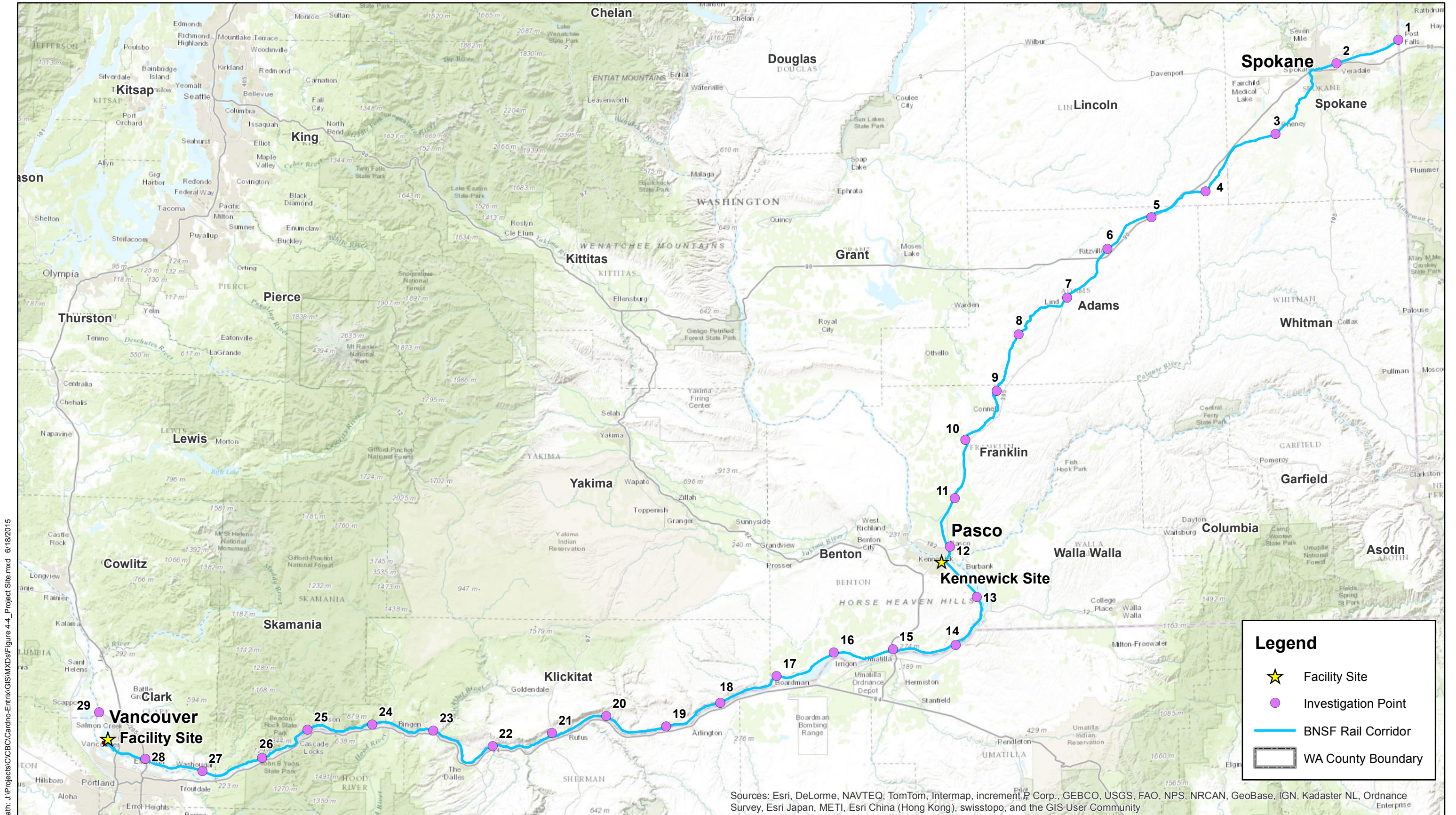
Figure 4-2
**Magnitude-Distance Deaggregation
 of 2,475-yr PGA Hazard**

PSH Deaggregation on NEHRP BC rock
 TSVEDT 122.718° W, 45.645 N.
 SA period 1.00 sec. Accel. ≥ 0.3699 g
 Ann. Exceedance Rate .412E-03. Mean Return Time 2475 yrs
 Mean (R,M, ϵ_0) 83.4 km, 8.25, 1.19
 Modal (R,M, ϵ_0) = 86.5 km, 9.00, 0.89 (from peak R,M bin)
 Modal (R,M, ϵ^*) = 86.5 km, 9.00, 1 to 2 sigma (from peak R,M, ϵ bin)
 Binning: DeltaR=10. km, deltaM=0.2, Delta ϵ =1.0



Source: USGS web site, <http://geohazards.usgs.gov/deagint/2008/>

Figure 4-3
**Magnitude-Distance Deaggregation
 of 2,475-yr S_a (1.0 sec) Hazard**



Legend

- ★ Facility Site
- Investigation Point
- BSNF Rail Corridor
- WA County Boundary

Figure 4-4

The project Site and BSNF Railroad Corridor



5 GROUND FAILURE HAZARDS

5.1 POTENTIAL FOR LIQUEFACTION-INDUCED GROUND DEFORMATION OR FAILURE

The potential for ground failure or excessive ground deformation hazards was examined at the near-shore portion of the project site (Area 400) and the on-shore portions of the site (Area 300 Tanks, Area 500 Pipeline) based on a combination of previous and current subsurface investigation data together with the results of commonly used technical analysis methods. The purpose of this effort was to provide an independent check of the similar efforts by the geotechnical consultants responsible for the current design of this project. The information available for this independent check includes SPT resistance values from traditional mud rotary borings, CPT tip and side friction resistance measurements, and shear-wave velocity measurements using a seismic cone penetrometer. The results of the evaluation are discussed in the following subsections for each of the three areas in question.

5.1.1 On-Shore - Areas 300 Tanks and 500 Pipeline

Each of the six 240-foot diameter tank locations was explored using a total of 7 to 9 drilled borings and cone penetrometer probes extending to depths up to 83 feet. The ground surface in this area ranges from about Elevation 26 to 30 feet. The borings were drilled by GRI in 2013 and 2014, and by Hayward Baker Inc. (HBI) in 2014. The cone penetrometer probes were advanced by GRI in 2013 and by HBI in 2014. These explorations have identified a soil profile consisting of an upper layer of medium dense to dense sandy fill extending to depths of 15 to 25 feet, typically followed by 5 to 15 feet of low to moderate plasticity silt to clayey silt in a soft to very soft condition, then medium dense sand extending to the top of the dense to very dense Troutdale Gravel. The depth to the top of the Troutdale ranges from roughly 50 to 65 feet below the ground surface, i.e. approximately Elevations -25 to -36 feet. A plot of SPT N-values versus elevation for most borings in the tank area is shown on Figure 5-1. The plot shows the sharp increase in N-values at the top of the Troutdale gravel layer, and also mostly indicates a dense zone in the sand layer just above the top of the Troutdale. It should be noted that occasional borings such as HB-B-104 show generally lower N-values in the sand layer until below about Elevation -25.

An evaluation of the likelihood of liquefaction at representative locations within Area 300 was performed using the LiquefyPro 5.8n software package from CivilTech Corporation (2009). Two boring locations (B-7, HB-B-108) and one CPT location (HB-CPT-145) were examined with this software, which uses the techniques identified in Youd and Idriss (1997). Two cases of ground motion for the evaluation were selected from the information presented in Section 4.3: (1) the first using the smaller magnitude ($M_w 6.5$) but higher PGA value (0.39g) for the MCE (2475-year return period) event from all other earthquakes besides the $M_w \geq 8$ CSZ events, and (2) the second using the higher magnitude ($M_w 8.9$) for the $M_w \geq 8$ CSZ events, but slightly lower PGA

value (0.34g). The results are presented on Figures A-1 to A-6 in Appendix A, and indicate generally negligible liquefaction and settlement below a depth of 45 feet (i.e. below Elevation -17). Liquefaction occurring above that level generated estimated settlements of approximately less than 1-inch to as much as 4.5 inches.

The possibility that lateral spread could reach the tanks from the Area 400 shoreline was also examined using the empirical method of Youd et al. (2002) for sloping or “free face” situations. In this case a free-face height of about 73 feet was used, which represents the elevation difference from the top of the shoreline (Elev 27) to the toe of the slope in the Columbia River (Elev -46). The analysis produced an estimated lateral spread magnitude of less than 2 feet at the location of the nearest tanks, which are about 2000 feet from the toe of the shoreline slope.

In Area 500 only 3 explorations appear to be available to assess the portion of transfer pipeline between the dock and the tanks. These explorations include GRI Boring B-21 near the north end, where the Troutdale is encountered at about Elevation -33, and Boring B-22 and cone probe CPT-5 near the center of that portion of transfer pipe, where the Troutdale is encountered at about Elev -41 and Elev -51, respectively. This trend of increasing depth to the dense Troutdale in the direction of the Columbia River is consistent with the bulk of exploration information in this vicinity.

5.1.2 Area 400 Marine Terminal (Dock and Adjacent Transfer Pipeline)

The most comprehensive presentation of existing conditions and previous subsurface investigation information at this location is provided in the GRI geotechnical reports of 2013 and 2014. The Figure 2 - Site Plan in the 2014 GRI report shows the locations of borings by Dames & Moore (1993) and borings/cone probes by GRI for the Tesoro Savage Energy Project, as well as details of the sloping topography of the shoreline. The ground surface elevations range from approximately Elevation 30 where the docks touch the shore at the top of the bank, down to a mudline at about Elevation -40, roughly 300 feet offshore from the top of the bank. The slope inclination between these two points starts at approximately 25 degrees (2H:1V) in the upper 10 feet, then flattens to about 8 degrees for a short distance before steepening again to an average of roughly 16 degrees (3.5H:1V) to the toe of the shoreline slope. In terms of lateral spread potential, this geometry amounts to a “free face” height of 73 feet. The soil profile down the slope appears to be granular fill to approximately Elevation 10, followed by a thick deposit of loose to medium dense native sand to typically Elevation -50 to -60 or below, where the very dense sandy gravel of the Troutdale Formation is encountered. It should be noted that the top of the Troutdale in the dock area ranges from Elevation -49 at GRI Boring B-24, to Elevation -69 at the location of Dames & Moore Boring B-1. The lower portion of the native sand layer appears to become dense for a thickness of approximately 4 to 6 feet, and this portion has been numerically identified as a separate less liquefaction-prone layer (Stratum 3b) in our evaluation. A plot of sampler N-values versus elevation for most borings in the Area 400 area is shown on

Figure 5-2, with a similar plot using N-values converted from CPT measurements presented in Figure 5-3.

Geotechnical information for most projects along the Columbia River within the Port of Vancouver property seems to indicate that the Troutdale Gravel slopes gently downward towards the centerline of the river. As Boring B-26, the most southerly of the explorations performed for this project, is still relatively close to the top of the shoreline embankment, the inclination of the Troutdale gravel is not well defined in the area most prone to lateral spreading. This boring indicates the top of the Troutdale is at Elevation -57 at that location. Other geotechnical information from projects in this area suggests that the top of the Troutdale at the toe of slopes along the northern shoreline of the river appears to slope downward to the west (downstream). Borings near the toe of the shoreline slope at Terminal 5, located approximately 2500 feet further downstream, have indicated the top of the Troutdale is roughly Elevation -110 (URS, 2011b). However, information from investigations at Berth 8 in Terminal 3 located 2500 feet upstream (L.R. Squire International, 1981; Dames & Moore, 1985) indicates that the top of the Troutdale there is at about Elevation -25 to -30 feet.

An evaluation of the likelihood of liquefaction at representative locations (boring locations B-23 & HB-B-109) within Area 400 was performed using the aforementioned LiquefyPro 5.8n software. The same two cases of ground motion mentioned in Section 5.1.1 were selected, except the PGA values were multiplied by 2/3 to obtain 0.22g for the M_w 8.9 for CSZ event and 0.26g for all other earthquakes. This scaling was done to be consistent with the requirements in the ASCE 41-16 standard. The results are presented on Figures A-7 to A-10 in Appendix A, and generally indicate very small zones of liquefaction throughout the soil profile when the smaller magnitude (M_w 6.5) event was considered. For the M_w 8.9 event, liquefaction to depths of up to 85 feet were estimated (i.e. to Elevation -57 to -58), with settlements of about 9 to 11 inches.

The lateral spread was estimated initially by the empirical method of Youd et al. (2002), and then by performing a slope stability analysis using Slope/W software by Geoslope International (2007). The PGA for these analyses were developed based on the ASCE 61-14 standard, Seismic Design of Piers and Wharves, which we understand will be used for the seismic design of the Area 400 terminal. The empirical analysis proceeded as described above in Section 5.1.1, and produced a lateral displacement of approximately 7 to 14 feet at the location of the Transfer Pipeline at 50 feet landward of the top of the shoreline embankment.

The Slope/W analysis was performed for static conditions using soil shear strength parameters estimated from SPT N-values. The result of the analysis is illustrated on Figure 5-3, which indicates the factor of safety is about 2.0, and hence confirms that the slope is stable for static conditions at the location of the Transfer Pipeline. The Slope/W analysis was also performed for the M_w 8.9 event using residual shear strength parameters for the liquefied soil, as well as a seismic horizontal coefficient, k_h , equal to 50 percent of the DE PGA (i.e., $k_h = 0.11$). The use of residual shear strength with the seismic coefficient was judged appropriate due to the expected

long duration of shaking for the M_w 8.9 event. The results of the analysis are illustrated on Figure 5-5, which indicates the factor of safety (FOS) under these circumstances is less than 0.40, and hence suggests that large displacements could occur at the location of the Transfer Pipeline. Accordingly, it will be important to establish a liquefaction mitigation approach that will be wide enough and deep enough to substantially increase the factor of safety and thus mitigate the potential for lateral spreading possibility at the Transfer Pipeline location along the top of the shoreline slope.

5.2 REVIEW OF PROPOSED MITIGATION DESIGN FOR GROUND DEFORMATION/FAILURES

Review comments on the appropriateness of the mitigation designs proposed by HBI (2015), and their methods of analysis used to obtain those designs, are provided below.

5.2.1 Area 300 Tanks and Area 500 Pipeline

Liquefaction mitigation in the tank area has been identified by HBI as consisting of installing 3-foot diameter stone columns on a square grid spaced at 8.2 feet apart to tip depths ranging from 35 to 40 feet, i.e., Elevations ranging from -14 to -18.5, per page 1 of the HBI (2015) report. The stone column lengths vary by specific tank location, although the “working surface” planned at Elevation 25 for all tanks (per Drawing Number HB-3 in the HBI report) means that at Tank 4 a stone column length shown at 36 feet results in a tip elevation of only Elev -11. AECOM recommends that a check be made on apparent discrepancies between planned tip elevations and soil conditions expected.

Downdrag loads on the stone columns due to consolidation of the soft silt/clayey silt layer have been considered in the design. Verification testing and additional mitigation, if needed, appears to be adequately addressed; the presence of the ground improvement efforts at the marine terminal appears to minimize the potential for lateral spread at the tank locations; and, the overall the potential for unsatisfactory performance of the tanks seems to be minor.

Along the north-south portion of the Transfer Pipeline (Area 500) where limited subsurface exploration information is available, the mitigation design is not clear, as Table 5 in the HBI (2015) report only indicates that tip elevations “varies” for the Transfer Pipeline, and Table 12 in that report only addresses the portion of the pipeline immediately adjacent to the tanks. The report text does indicate that stone columns supporting the Transfer Pipeline will have tips ranging from “about Elevation -5 to about Elevation -16”. The currently available subsurface information suggests that stone column depths will need to be deeper as the pipeline nears the Marine Terminal, because the depth to non-liquefiable sands and Troutdale gravel is increasing. AECOM requests that further elaboration of the Area 500 pipeline foundation support be provided.

5.2.2 Area 400 Marine Terminal

Liquefaction mitigation in the marine terminal area has been identified by HBI as consisting of three methods, including (1) vibroreplacement stone columns, (2) jet grout columns, and (3) deep soil mix (DSM) panels. As currently described, the mitigation seems to rely most heavily on the stone columns, and the overall performance objectives are ambitious, including limiting vertical (settlement) and lateral displacements to 2-inches or less. The bank of stone columns along the shoreline is shown penetrating to approximately Elevation -53. As illustrated on Drawing HB-14, the stone columns are supplanted by 100 percent jet grout column installation near the top of the shoreline embankment at the eastern-most dock. Elsewhere, the stone columns are supported on the onshore side by a system of jet-grout, column-supported, DSM panels that directly support the Transfer Pipeline. A depiction of the ground improvement design elements is shown on Figure 5-6. It should be noted that there is no well-established seismic performance record of the DSM panels supported on jet grout columns.

The description of the installation and verification testing procedures is comprehensive, including CPT probes to verify densification and load testing of improved ground.

AECOM recommends that the currently planned stone column tip elevation level (Elev -53) be reconsidered in light of the apparently significant number of explorations where the top of the dense Troutdale gravel layer is Elevation -55 or deeper. Also, there is uncertainty that the lower portion of the overlying sand is sufficiently dense to prevent liquefaction at those increased depths. Alternatively, the stone column installation procedure could include a requirement that the penetration rate/resistance of the vibratory probe be set to match that where stone columns were installed at the location of explorations where dense sand was clearly identified at the stone column termination depth.

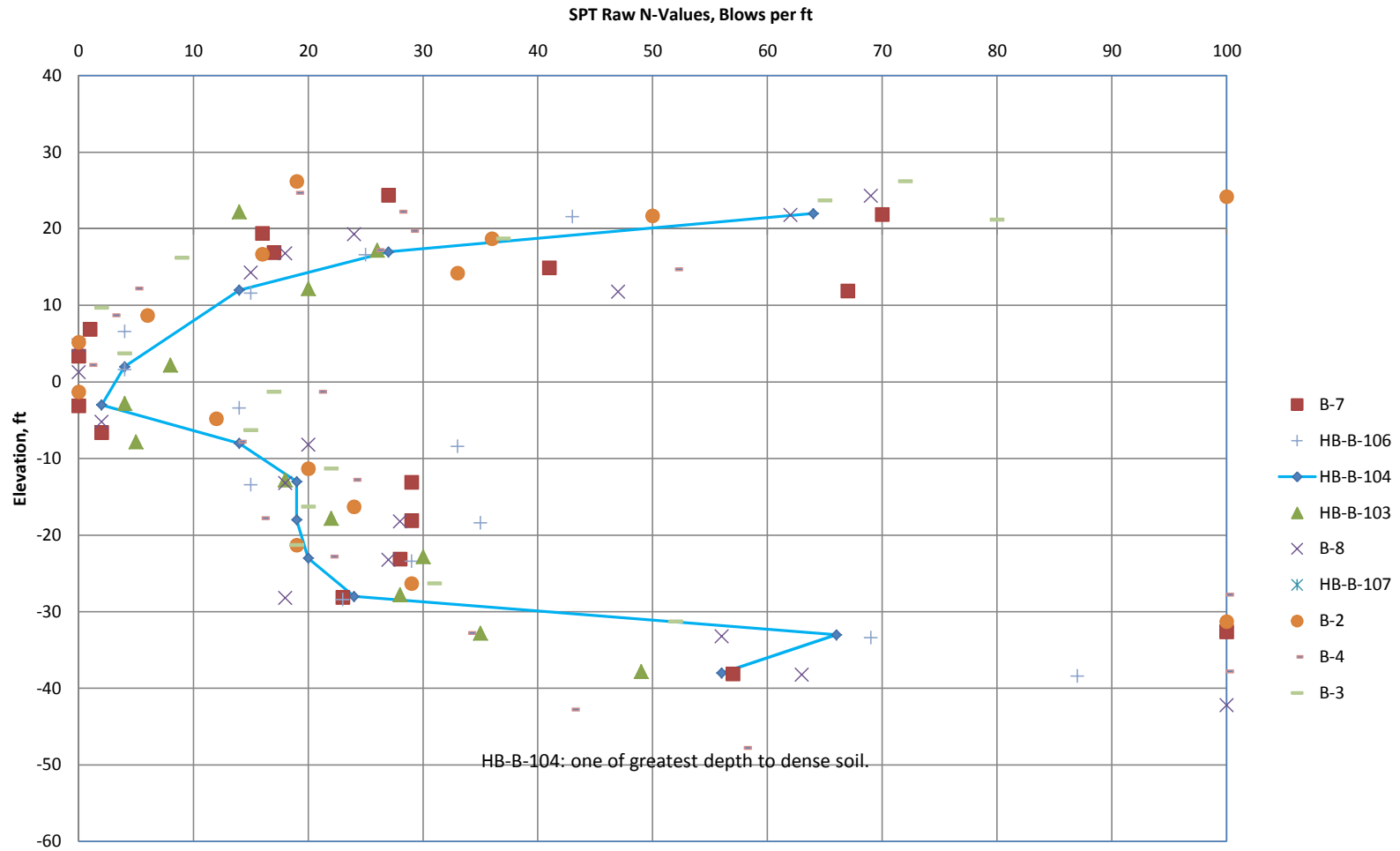
As the potential for sliding of the embankment slope is expected to remain high, even after the multiple ground improvement efforts are completed at the top of the embankment, the possibility will still exist for ground displacement and concurrent movement of the moored ship at the end of the dock. That movement could in turn produce a release of petroleum if the transfer system from the vessel is not sufficiently flexible. AECOM recommends that this release potential be further evaluated, and appropriate resolutions identified, as further discussed in Section 7 of this report.

6 TSUNAMI AND SEICHE HAZARDS

Tsunamis are water waves generated in oceanic areas by (1) earthquakes (typically subduction) that displace the seafloor, (2) submarine landslides that may or may not be induced by earthquakes, or (3) offshore volcanic eruptions that displace large volumes of seawater, such as the 1883 Krakatoa eruption in Indonesia. The CSZ and more distant subduction zones can generate tsunamis that would impact the Pacific Northwest Coast. For example, the 1964 Alaska Earthquake of M_w 9.2 generated a large tsunami that impacted the Pacific Northwest Coast and caused significant damage to the coastal town of Crescent City, California. Pre-historic (paleo) tsunami deposits interpreted to be associated with CSZ earthquakes have been identified and dated at multiple locations along the Oregon and Washington coast.

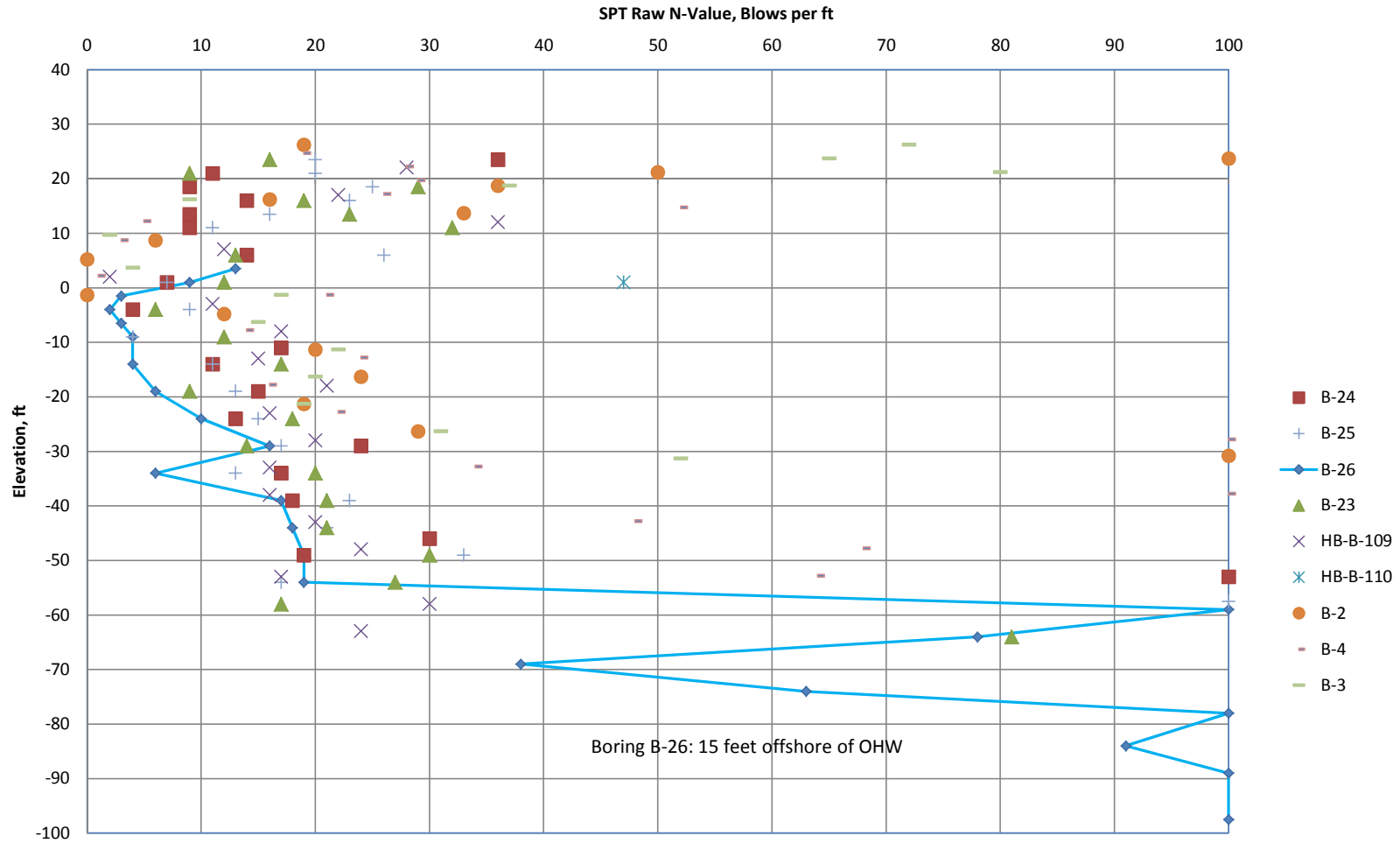
The TSVEDT site is approximately 103.5 miles up the Columbia River from the Pacific Coast and is at approximately Elevation 25 to 35 feet (NGVD). Tsunamis are not considered a potential hazard at the site based on the distance of the coast to the site, the changes in direction of the Columbia River from its mouth to the site, the elevation of the site, and modeling of tsunami inundation associated with a CSZ great earthquake (DOGAMI 2015b; Walsh et al. 2000).

Seiches are earthquake-generated waves that can occur in inland bodies of water, including rivers. After the 1964 Alaska earthquake, very minor (less than 1 foot) seiches were reported in the upper (non-free flowing) section of the Columbia River system from McNary Reservoir (McNary Dam) to Franklin D. Roosevelt Lake (Grand Coulee Dam) (McGarr and Vorhis 1968). No historical seiches are known from the lower, free-flowing Columbia River where the TSVEDT site is located. The likelihood that seiche could affect the TSVEDT site is very low.



Note: Soil information based on boring logs at Tank Area.

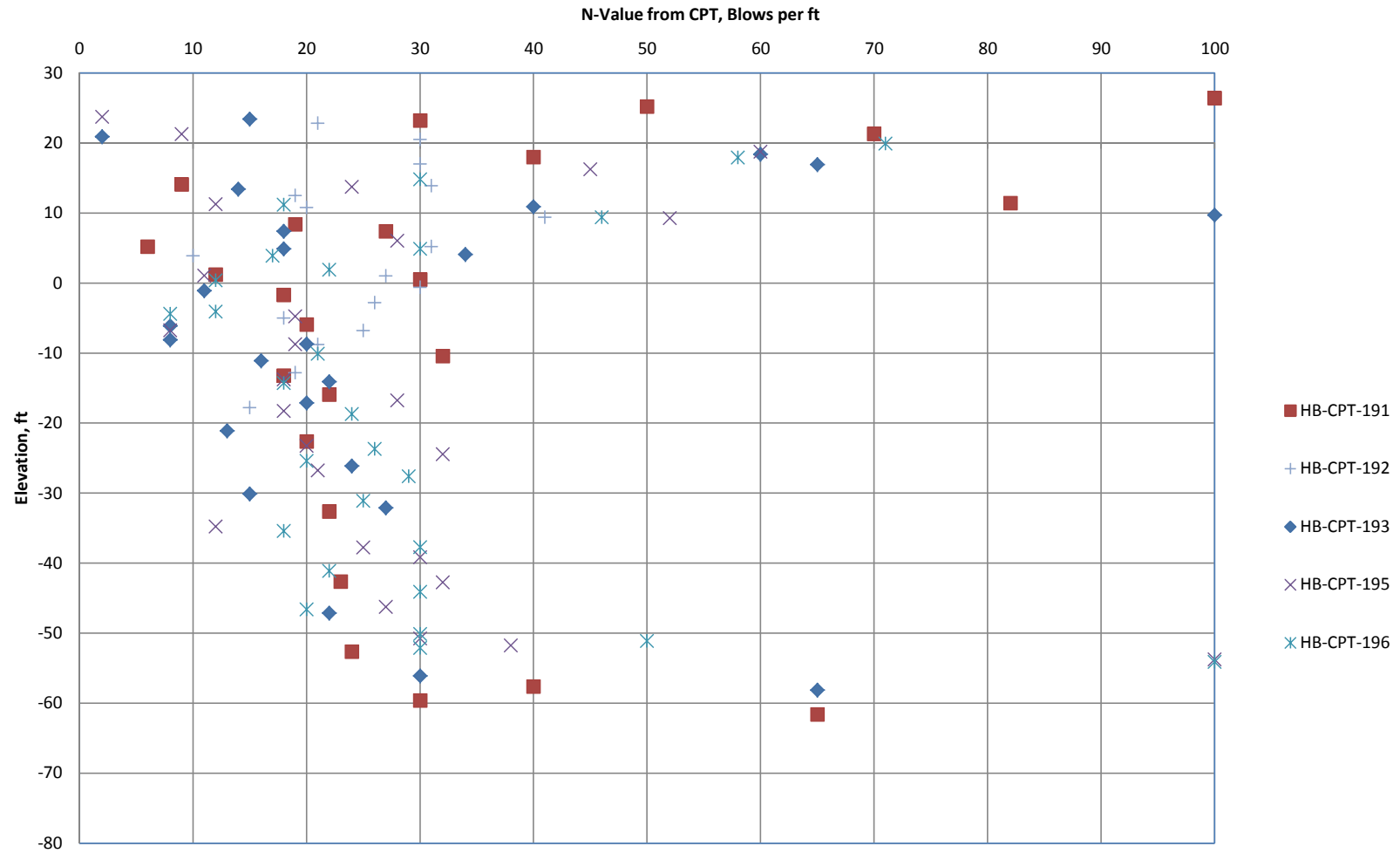
Figure 5-1
SPT N-Values of Borings vs. Elevations, Area 300 Tank Area



Notes:

1. Soil information based on near shore boring logs.

Figure 5-2
SPT N-Values of Borings vs. Elevations, Area 400 Dock



Notes:

- 1. Soil information based on near shore CPT logs.

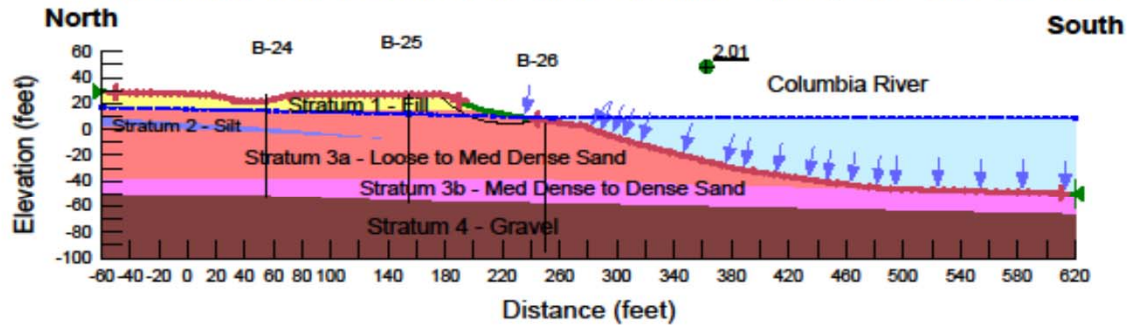
Figure 5-3
N-Values from CPTs vs. Elevations, Area 400 Dock

**Tesoro Savage Terminal
Area 400 Dock Area
Seismic Coefficient: $k_h = 0$**

FOS = 2.01

Date: 6/8/2015
File Name: Static Section BB.gsz

Name: Existing Fill Model: Mohr-Coulomb Unit Weight: 120 Cohesion: 0 Phi: 38 Piezometric Line: 1
 Name: Stratum 2 - Silt Model: Undrained (Phi=0) Unit Weight: 115 Cohesion: 650 Piezometric Line: 1
 Name: Stratum 3a - Loose to Med Dense Sand Model: Mohr-Coulomb Unit Weight: 115 Cohesion: 0 Phi: 34 Piezometric Line: 1
 Name: Stratum 4 - Gravel Model: Mohr-Coulomb Unit Weight: 130 Cohesion: 0 Phi: 42 Piezometric Line: 1
 Name: Stratum 3b - Med. Dense to Dense Sand Model: Mohr-Coulomb Unit Weight: 120 Cohesion: 0 Phi: 36 Piezometric Line: 1



Note: Soil information based on boring logs at Area 400 Dock Area.

Figure 5-4
Slope Stability Analysis Results - Static State, Area 400 Dock

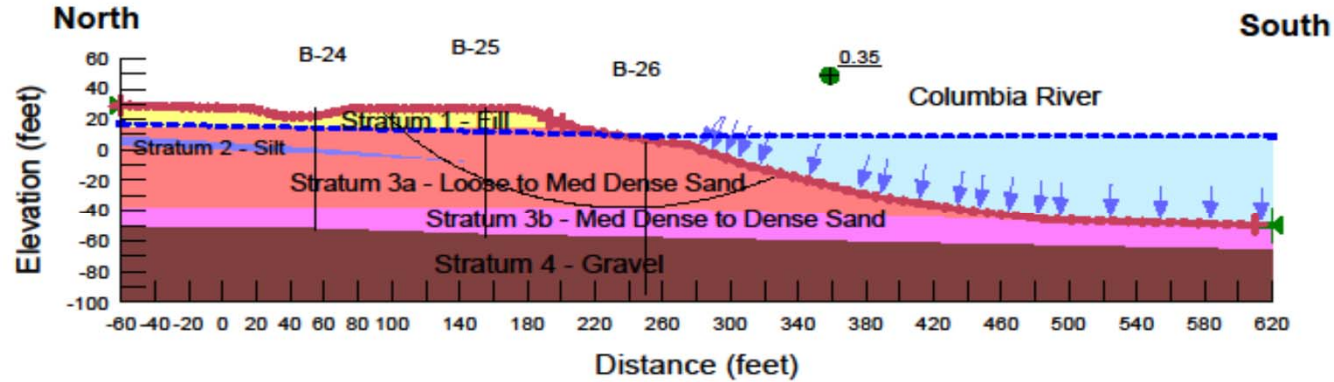
**Tesoro Savage Terminal
Area 400 Dock Area
Seismic Coefficient: $kh = 0.11$**

FOS = 0.35

Date: 6/8/2015

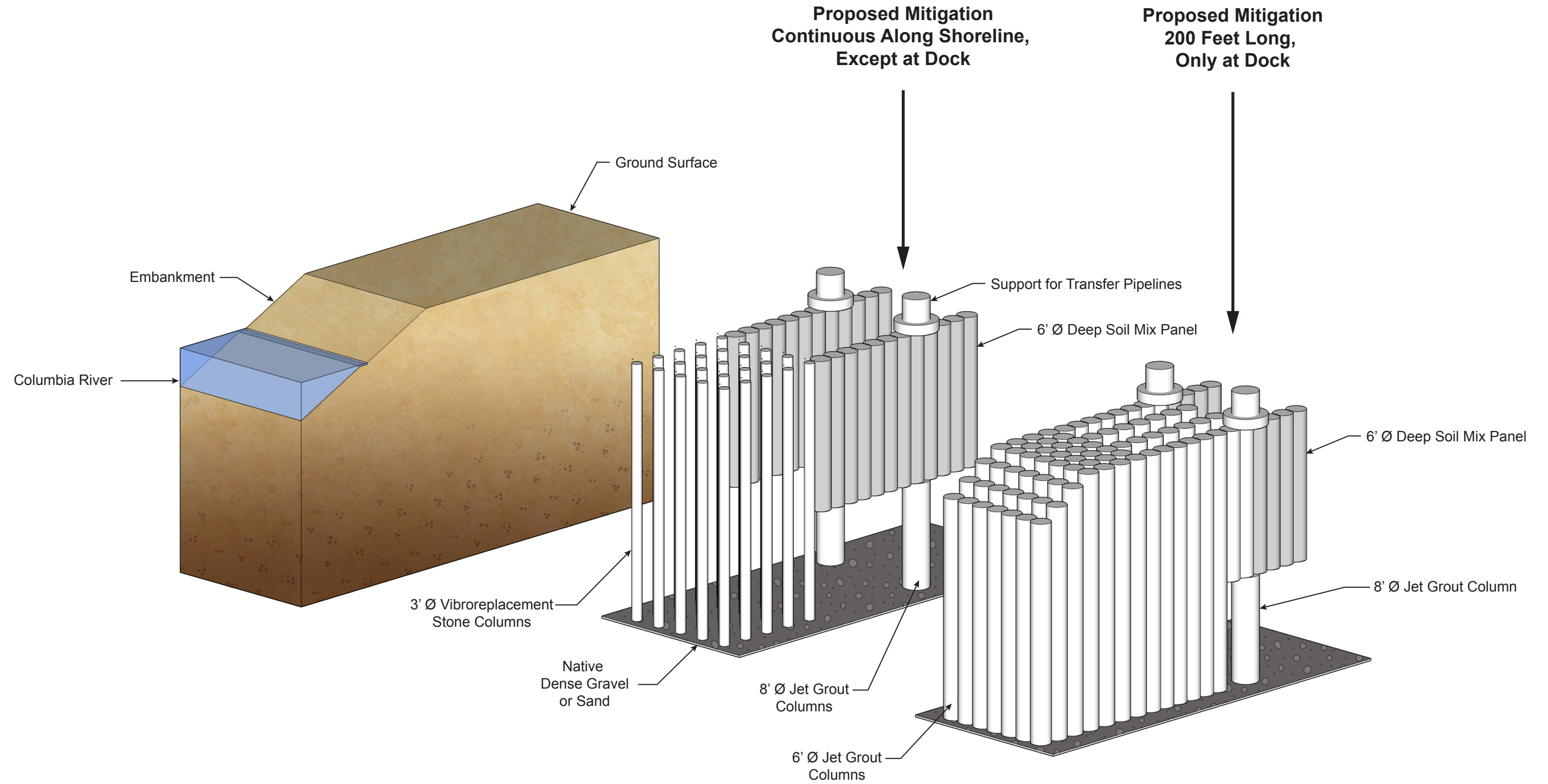
File Name: Seismic Section BB - kh.gsz

Name: Existing Fill Model: Mohr-Coulomb Unit Weight: 120 Cohesion: 0 Phi: 38 Piezometric Line: 1
 Name: Stratum 2 - Silt Model: Undrained (Phi=0) Unit Weight: 115 Cohesion: 650 Piezometric Line: 1
 Name: Stratum 3a - Loose to Med Dense Sand Model: Mohr-Coulomb Unit Weight: 115 Cohesion: 290 Phi: 0 Piezometric Line: 1
 Name: Stratum 4 - Gravel Model: Mohr-Coulomb Unit Weight: 130 Cohesion: 0 Phi: 42 Piezometric Line: 1
 Name: Stratum 3b - Med. Dense to Dense Sand Model: Mohr-Coulomb Unit Weight: 120 Cohesion: 930 Phi: 0 Piezometric Line: 1



Note: Soil information based on boring logs at Area 400 Dock Area.

Figure 5-5
Liquefied Slope Stability Analysis Result - Pseudo-Static ($ky = 0.11$), Area 400 Dock



Note: For clarity, soil inbetween Vibroreplacement Stone Columns and Jet Grout Columns is not shown.

7 SEISMIC DESIGN CONSIDERATIONS

7.1 Design for Ground Motion

7.1.1 Above Ground Structures

The seismic design of the various above-ground structures and components of the proposed TSVEDT facility for loads generated by earthquake ground motion alone would be accomplished using applicable codes and standards.

The upland above-ground facilities, other than the oil storage tanks, would meet the provisions of IBC 2012, which incorporates the ASCE 7-10 standard by reference.

The oil storage tanks (Area 300) would be designed to the seismic provisions in Annex E of the 12th edition of the API 650 standard, which is aligned with the ASCE 7-10 standard.

On the other hand, the seismic design of piers and wharves not accessible to the general public is beyond the scope of the ASCE 7-10 standard. For these structures in the Marine Terminal (Area 400), the recently released ASCE 61-14 standard, Seismic Design of Piers and Wharves, can be used for the seismic design. The Design Earthquake (DE) in this standard is taken from the ASCE 7-05 standard, not the ASCE 7-10 standard, even though the ASCE 7-10 standard was already published. The main reason the committee developing the ASCE 61-14 standard did not adopt ASCE 7-10 was the requirements for liquefaction assessment in ASCE 7-05 were less onerous than those in ASCE 7-10. ASCE 7-05 permits the evaluation to be conducted for the DE PGA, which is two-thirds (2/3) of the MCE_G PGA, whereas ASCE 7-10 requires the evaluation to be conducted for the MCE PGA.

The Applicant has indicated that in the areas where the structures and pipelines will be located, the liquefaction potential will be mitigated through soil improvement. This improvement will likely not increase the shear-wave velocity of the improved soils enough to place them into Site Class C. Thus, the surface ground motion would correspond to Site Class D, and the associated DE spectral response acceleration parameters that would be used in the absence of a site-specific ground-motion study would be those listed in Table 7-1.

**Table 7-1
DE Spectral Response Acceleration Parameters for Site Class D**

Facility	S_{DS}	S_{D1}
Upland facilities (ASCE 7-10 & API 650, Annex E)	0.705	0.436
Marine Terminal (ASCE 61-14 & ASCE 7-05)	0.703	0.385

These parameters define short and intermediate segments of the DE Design Response Spectrum (see Figure 11.4-1 in the ASCE 7-10 standard) used to compute the earthquake loads. The T_L parameter in this figure defines the natural period (T) where this DE spectrum transitions from constant spectral velocity to constant spectral displacement. A value of T_L for the site is 16 sec, and it was based on the potential for $M \geq 8$ earthquakes on the CSZ (Crouse et al., 2006).

According to the Applicant, the Design Classification of the Terminal structures, per ASCE 61-14, is Moderate, which means the seismic design would be done for a Contingency Level Earthquake (CLE) in addition to the DE. For the Moderate classification, the CLE is the ground motion with a return period of 224 years. The corresponding response spectral values from the 2002 USGS ground-motion data, adjusted by the appropriate site coefficients for Site Class D, are: $PGA = 0.196g$, $S_a(0.2 \text{ sec}) = 0.459g$, and $S_a(1.0 \text{ sec}) = 0.230g$.

7.1.2 Buried Pipelines

Codes or standards (similar to the ASCE 7 or IBC) for seismic design of buried oil and gas pipelines do not exist. However, two well-known guidelines documents (ASCE, 1984; PRCI, 2003) can be used to analyze the buried segment of the oil pipeline and the existing buried gas pipeline, which may be replaced due to rerouting.

The calculation of strains in straight sections of the pipelines involves simple equations based on wave-propagation principles and the assumption that the pipeline does not interact with the surrounding soil. The ground-motion parameter that produces by far the greatest strain is the maximum ground velocity, V_{max} , which can be estimated as the 5% damped, horizontal component of response spectral acceleration at 1.0-sec period, $S_a(1.0 \text{ sec})$, divided by 1.65, a conversion factor from Newmark and Hall (1982). Some recent projects have used the 2475-yr value for $S_a(1.0 \text{ sec})$ to be consistent with the MCE in the ASCE 7-05 standard.

The ASCE (1984) guidelines also provide methods to analyze seismic induced stresses at sharp bends in the pipeline.

7.2 Design for Permanent Ground Deformation

The analysis in Section 5 clearly confirms that soil improvement will be required at key locations of the TSVEDT site in order to meet the performance objectives for the facility. There are no codes stating the requirements the various soil-improvement methods must satisfy to mitigate the potential for liquefaction and the attendant settlements and lateral spreading, but *in situ* testing (e.g., CPT and shear-wave velocity surveys) can verify whether the soil has been sufficiently improved to achieve adequate factors of safety against liquefaction. The soil-improvement method selected should allow for the possibility that the improved soil does not meet the verification criteria and that further soil improvement can be made, as necessary.



In the Area 400 Marine Terminal, where the liquefaction hazard is greatest, the stone columns will need to extend either to the dense zone at the base of the sand layer or to the dense Troutdale gravel, and the installation method must be monitored to achieve this depth.

In addition to pseudo-static methods of stability analysis, nonlinear dynamic analyses using numerical models (e.g., FLAC, PLAXIS) are recommended to analyze the Marine Terminal in its improved soil state. Simple models of the marine structures should be included to account for inertial loads due to soil-structure interaction. The results from both pseudo-static and dynamic methods would provide more confidence in the design.

However, it should be remembered that in the Marine Terminal area, the ground-improvement design offers protection to the most critical element of the transfer system, i.e. the pipeline carrying the petroleum product, but that embankment slope failure on the river side of the stone columns is likely to occur during seismic shaking. The slope failure could move the dock and ship further from the shore and hence affect the integrity of the oil-transfer system from the onshore transfer pipeline to the ship. Soil-improvement on the embankment and offshore is more difficult. The installation of additional piles along the embankment in the docking area is one option to help mitigate the potential for lateral spreading. Methods to design the piles supporting the dock structure are available. Also, flexibility in the oil-transfer system would alleviate the possibility that the connection to the storage container on the ship would be severed.

8 CONCLUSIONS

Based on the information presented in this report, AECOM concludes that the hazards at the TSVEDT site due to tsunami and seiche are negligible.

The ground-rupture hazard at the TSVEDT site due to faulting is also negligible based on the locations and projections of the Quaternary faults mapped in the site vicinity (Figure 2-4).

The ground-motion hazard at the site is moderate to high, but design to applicable seismic codes and standards will mitigate the risk to the various structures and components comprising the TSVEDT facility, provided the potential for permanent ground deformation is mitigated. Although the design to these codes and standards will minimize the risk of damage, it will not necessarily eliminate it - a common misperception among owners.

The probabilistic MCE_R ground motions in the ASCE 7-10 standard were established based on (1) a nominal 1% probability of structural failure in a 50-yr period, and (2) a 10% probability of structural failure given the occurrence of the MCE_R ground motions. Thus, if MCE_R ground motions were to occur at the site, then significant damage might result that could cause a shutdown of the facility until repairs were made.

More likely the ground motions during an assumed 50-yr period of operation will be much less than the MCE_R ground motions. In this case, the damage, if any, should be minimal with no loss of operation.

As noted in Section 7.1.1, the criteria for liquefaction and soil stability assessments per the ASCE 7-05 standard, incorporated by reference into the ASCE 61-14 standard, are less onerous for the Marine Terminal than for the upland portion of the facility. Thus, the seismic risk at the terminal may be greater. If the Applicant elects to design the soil improvement at the Marine Terminal to mitigate potential slope failure for only the DE motion (= 2/3 MCE motion), as required by the ASCE 7-05 standard, then a check of the stability for the MCE would be prudent.

In any case, if the earthquake shaking does cause catastrophic failure of one or more of the oil storage tanks, then berms surrounding the tanks should have adequate factors of safety to remain intact in order to contain the spill. Likewise, the flow through a ruptured pipeline should be shutdown automatically so the leak volume is minimized. The facility operator should not count on external power sources for this task, since there may be a region-wide power outage during the earthquake. The facility should be equipped with emergency power generators that can perform the shutdown.

9 REFERENCES

- ASCE, 1984. Guidelines for the Seismic Design of Oil and Gas Pipeline Systems. Prepared by the committee on Gas and Liquid Fuels Lifelines of the ASCE Technical Council on Lifeline Earthquake Engineering, American Society of Civil Engineers, New York, New York, 473 p.
- Atwater, B.F., and Griggs, G.B., 2012, Deep-sea turbidites as guides to Holocene earthquake history at the Cascadia Subduction Zone—Alternative views for a seismic-hazard workshop: U.S. Geological Survey Open-File Report 2012-1043, 58 p., <http://pubs.usgs.gov/of/2012/1043/>.
- Atwater, B.F., Nelson, A.R., Clague, J.J., Carver, G.A., Bobrowsky, T., Bourgeois, J., Darienzo, M.E., Grant, W.C., Hemphill-Haley, E., Kelsey, H.M., Jacoby, G.C., Nishenko, S.P., Palmer, S.P., Peterson, C.D., Reinhart, M.A., and Yamaguchi, D.K., 1995, Summary of coastal geologic evidence for past great earthquakes at the Cascadia subduction zone, *Earthquake Spectra*, v. 11, p. 1–18.
- Atwater, B.F., Musumi-Rokkaku, S., Satake, K. Tsuji, Y., Ueda, K., and Yamaguchi, D.K., 2005, The orphan tsunami of 1700—Japanese clues to a parent earthquake in North America, U.S. Geological Survey Professional Paper 1707, 133 p. (published jointly by University of Washington Press, Seattle).
- Atwater, B.F., Carson, B., Griggs, G.B., Johnson, H.P., and Salmi, M.S., 2014, Rethinking turbidite paleoseismology along the Cascadia subduction zone, *Geology*, v. 42, no. 9 p. 827-830, doi: 10.1130/G35902.1
- Bakun, W.H., Haugerud, R.A., Hopper, M.G., and Ludwin R.S., 2002, The December 1872 Washington State earthquake, *Bulletin of the Seismological Society of America*, v. 92, no. 8, p. 3239-3258.
- Barnett, E.A., Haugerud, R.A., Sherrod, B.L., Weaver, C.S., Pratt, T.L., and Blakely, R.J., 2010, Deformation in the Puget Lowland, Washington, U.S. Geological Survey, Open-File Report 2010-1149, 32 p. and 14 maps.
- Barnett, E.A., Sherrod, B.L. Norris, R., and Gibbons, D., 2013, Paleoseismology of a Newly Discovered Scarp in the Yakima Fold-and-Thrust Belt, Kittitas County, Washington, U.S. Geological Survey, Scientific Investigations Map 3212.
- Blais-Stevens, A., Rogers, G.C., and Clague, J.J., 2011, A revised earthquake chronology for the last 4000 years inferred from varve-bounded debris-flow deposits beneath an Inlet near Victoria, British Columbia, *Bulletin of the Seismological Society of America*, v. 101, no. 1, p. 1-12.
- Blakely, R.J., Sherrod, B.L., Weaver, C.S., Wells, R.E., and Rohay, A.C., 2014, The Wallula fault and tectonic framework of south-central Washington, as interpreted from magnetic and gravity anomalies, *Tectonophysics*, v. 624–625, p. 32–45.



Burns, W.J. and nine co-authors, 2012, Multi-Hazard and Risk Study of the Mount Hood region, Multnomah, Clackamas, and Hood River Counties, Oregon, Oregon Department of Geology and Mineral Industries, Open-File Report O-11-16.

CivilTech Corporation, 2009, LiquefyPro Software.

Czajkowski J.L. and J.D. Bowman, 2014, Faults and Earthquakes in Washington State, Washington Division of Geology and Earth Resources, Open File Report 2014-05

Clague, J.J., Bobrowsky, P.T., and Hutchinson, I., 2000, A review of geological records for large tsunamis at Vancouver Island, British Columbia and implications for hazard, Quaternary Science Reviews, v. 19, p. 849-863.

Crouse, C.B., Leyendecker, E.V., Somerville, P.G., Power, M., and Silva, W.J., 2006, Development of seismic ground-motion criteria for the ASCE 7 standard, Proceedings of the 8th U.S. National Conference on Earthquake Engineering, Paper No. 533, San Francisco, CA, April.

Dames & Moore, 1985, Report of Geotechnical Investigation, Proposed Berth 8 Expansion, Port of Vancouver, WA.

Dames & Moore, 1993, Geotechnical Investigation, Proposed T-Docks/Dolphins, Port of Vancouver Washington.

Geo-slope International Ltd., 2007, SLOPEW Software.

Goldfinger, C., Nelson, C.H., Morey, A., Johnson, J.E., Patton, J., Karabanov, E., Gutierrez-Pastor, J., Eriksson, A.T., Gracia, E., Enkin, R., Dallimore, A., Dunhill, G., and Vallier, T., 2012, Turbidite Event History: Methods and Implications for Holocene Paleoseismicity of the Cascadia Subduction Zone, U.S. Geological Survey Professional Paper 1661-F, 184p.

Goldfinger, C., Morey, A.E., Black, B., Beeson, J., Nelson, C.H., and Patton, J., 2013, Spatially limited mud turbidites on the Cascadia margin: segmented earthquake ruptures? Natural Hazards and Earth Systems Science, v. 13, p. 2109–2146, doi:10.5194/nhess-13-2109-2013.

GRI, 2013, Geotechnical Investigation, Tesoro Savage Vancouver Energy Distribution Terminal – Upland Facility, Port of Vancouver, USA. Report submitted to BergerABAM, December 20.

GRI, 2014, Geotechnical Investigation, Tesoro Savage Energy Distribution Terminal–Dock Facility, Port of Vancouver, WA.

Hayward Baker, Inc. (HBI), 2015, Vancouver Energy Terminal, Ground Improvement Design – Areas 300 & 400. Report submitted to R&M Engineering Consultants, April 15.

- Ichinose, G. A., H. K. Thio, and P. G. Somerville, 2004, Rupture process and near-source shaking of the 1965 Seattle-Tacoma and 2001 Nisqually, intraslab earthquakes, *Geophysical Research, Letters*, v. 31, L10604, doi:10.1029/2004GL019668
- Kelsey, H.M., Nelson, A.R., Hemphill-Haley, E., and Witter, R., 2005, Tsunami history of an Oregon coastal lake reveals a 4600 yr record of great earthquakes on the Cascadia subduction zone, *Geological Society of America Bulletin*, v. 117, p. 1009–1032.
- Kelsey, H.M., Sherrod, B. L., Nelson, A.R., and Brocher, T.M., 2008, Earthquakes generated from bedding plane-parallel reverse faults above an active wedge thrust, Seattle fault zone *Geological Society of America Bulletin*, v. 120, no. 11/12, p. 1581–1597, doi: 10.1130/B26282.1
- Lidke, D.J., Johnson, S.Y., McCrory, P.A., Personius, S.F., Nelson, A.R., Dart, R.L., Bradley, L., Haller, K.M., and Machette, M.N., 2003, Map and data for Quaternary faults and folds in Washington, U.S. Geological Survey Open-File Report 03-428.
- L.R. Squier Inc., 1981, Geotechnical Investigation, Proposed Berth #8 Extension, Port of Vancouver, WA.
- Mabey, M.A., I. P. Madin, T.L. Youd and C.F. Jones, 1993, Oregon Department of Geology and Mineral Industries: MS-79. EQ hazard maps of Portland quad, Multnomah and Washington Cos., OR and Clark Co., WA, 98 p., 3 pls., 1:24,000
- McCaffrey, R., Qamar, A.I., King, R.W., Wells, R.E., Ning, Z., Williams, C.A., Stevens, C.W., Vollick, J.J., and Zwick, P.C., 2007, Fault locking, block rotation, and crustal deformation in the Pacific Northwest, *Geophysical Journal International*, v. 169, p. 1315–1340.
- McCaffrey, R., King, R.W., Payne, S.J., and Lancaster, M., 2013, Active tectonics of northwestern U.S. inferred from GPS-derived surface velocities, *Journal of Geophysical Research*, v. 118, p. 709–723, doi:10.1029/2012JB009473.
- McGarr, A. & Vorhis, R.C., 1968, Seismic seiches from the March 1964 Alaska earthquake, U.S. Geological Survey Professional Paper 544-E, p. E1-E43, 1 sheet, scale 1:5,000,000.
- Myers, B. and Driedger, C., 2008, Eruptions in the Cascade Range During the Past 4,000 Years U.S. Geological Survey, General Information Product G3
- Nelson, A.R., Kelsey, H.M., and Witter, R.C., 2006, Great earthquakes of variable magnitude at the Cascadia subduction zone *Quaternary Research*, v. 65, p. 354–365.
- Nelson, A.R., Personius, S.F., Buck, J., Bradley, L., Sherrod, B.L., Henley, G., II, Liberty, L.M., Kelsey, H.M., Witter, R.C., Koehler, R.D., III, and Schermer, E.R., 2008, Field and laboratory data from an earthquake history study of scarps in the hanging wall of the Tacoma fault, Mason and Pierce Counties, Washington: U.S. Geological Survey Scientific Investigations Map 3060, <http://pubs.er.usgs.gov/usgspubs/sim/sim3060>.

Nelson, A.R., Personius, S.F., Sherrod, B.L., Kelsey, H.M., Johnson, S.Y., Bradley, L. and Wells, R.E., 2014, Diverse rupture modes for surface-deforming upper plate earthquakes in the southern Puget Lowland of Washington State, *Geosphere*, published online June 24, 2014, doi: 10.1130/GES00967.1

Newmark, N.M., and Hall, W.J., 1982. *Earthquake Spectra and Design*. Monograph, Earthquake Engineering Research Institute, Berkeley, California.

Oregon Department of Geology and Mineral Industries, 2014, Statewide Landslide Information Database v. 3.2, <http://www.oregongeology.org/sub/slido/index.htm>

Oregon Department of Geology and Mineral Industries, 2015a, Database and GIS file of Oregon Active Faults, <http://www.oregongeology.org/sub/gtilo/data/ORActiveFault.zip>.

Oregon Department of Geology and Mineral Industries, 2015b, Oregon HazVu: Statewide GeoHazards Viewer, <http://www.oregongeology.org/hazvu/>

Personius, S.F., Dart, R.L., Bradley, L., and Haller, K.M., 2003, Map and data for Quaternary faults and folds in Oregon, U.S. Geological Survey Open-File Report 03-095.

Petersen, M.D., and 14 coauthors, 2008, Documentation for the 2008 Update of the United States National Seismic Hazard Maps, USGS Open-File Report 2008-1128.

Petersen, M.D., and 16 coauthors, Documentation for the 2014 Update of the United States National Seismic Hazard Maps, USGS Open-File Report 2014-1091.

Phillips, W.M., 1987, *Geologic Map of the Vancouver Quadrangle, Washington and Oregon*, Washington Department of Natural Resources, Division of Geology and Earth Resources, Open File Report 87-10.

PRCI, 2004. *Guidelines for the Seismic Design and Assessment of Natural Gas and Liquid Hydrocarbon Pipelines*. Prepared for Pipeline Design, Construction & Operations Technical Committee of Pipeline Research Council International, Inc. Prepared by D.G. Honegger Consulting, and D.J. Nyman and Associates, October 1.

Satake, K., Shimazaki, K., Tsujit, Y. and Ueda, B.K., 1996, Time and size of a giant earthquake in Cascadia inferred from Japanese tsunami records of January 1700, *Nature*, v. 379, p. 246-249.

Satake, K., Wang, K., and Atwater, B.F., 2003. Fault slip and seismic moment of the 1700 Cascadia earthquake inferred from Japanese tsunami descriptions, *Journal of Geophysical Research*, v. 108, no. B11, p. 2535, doi:10.1029/2003JB002521).

Sherrod, B. L., 2015, Lidar identifies source for 1872 earthquake near Chelan, Washington, *Seismological Research Letters*, v. 86, No. 2B, p. 608.

Sherrod, B.L., Bucknam, R.C., and Leopold, E.B., 2000, Holocene relative sea level changes along the Seattle fault at Restoration Point, Washington: *Quaternary Research*, v. 54, p. 384–393, doi: 10.1006/qres.2000.2180

Sherrod, B.L., Barnett, E.A., Knepprath, N., and Foit, F.F., Jr., 2013, Paleoseismology of a possible fault scarp in Wenas Valley, central Washington: U.S. Geological Survey Scientific Investigations Map 3239.

URS Corporation, 2011a, Final Report of Seismic Hazard Study, Terminal 5 Bulk Handling Facility, Port of Vancouver, WA.

URS Corporation, 2011b, Report of Geotechnical Investigation, Terminal 5 Bulk Handling Facility, Port of Vancouver, WA.

U.S. Geological Survey, 2006, Quaternary fault and fold database for the United States, accessed Jan 9, 2015, from USGS web site: <http://earthquakes.usgs.gov/regional/qfaults/>

Walsh, T.J., C.G. Caruthers, A.C. Heinitz, E.P. Myers III, A.M. Baptista, G.B. Erdakos, and R.A. Kamphaus, 2000, Tsunami Hazard Map of the Southern Washington Coast--Modeled Tsunami Inundation from a Cascadia Subduction Zone Earthquake, Washington Division of Geology and Earth Resources, Geologic Map GM-49.

Washington Division of Geology and Earth Resources, 2013, Washington State seismogenic features–GIS data, August, 2013.
(http://www.dnr.wa.gov/Publications/ger_portal_seismogenic_features.zip)

Washington Division of Geology and Earth Resources, 2014, Washington State landslides and landforms–GIS data, December, 2014: Washington Division of Geology and Earth Resources Digital Data Series DS-12, version 2.0.
[http://www.dnr.wa.gov/publications/ger_portal_landslides_landforms.zip]

Wells, R.E., and R.McCaffrey, 2013, Steady rotation of the Cascade arc, *Geology*, v. 41, p. 1027-1030, doi: 10.1130/G34514.1

Wells, R.E., Weaver, C.S., and Blakely, R.J., 1998, Forearc migration in Cascadia and its neo tectonic significance: *Geology*, v. 26, p. 759–762, doi:10.1130/0091-7613(1998)026<0759:FAMICA>2.3.CO;2.

Wells, R.E., Blakely, R.J., and Weaver, C.S., 2002, Cascadia microplate models and within-slab earthquakes, in S. Kirby, K. Wang, and S. Dunlop (eds.), *The Cascadia Subduction Zone and Related Subduction Systems Seismic Structure, Intraslab Earthquakes and Processes, and Earthquake Hazards*: U.S. Geological Survey Open-File Report 02-328 and Geological Survey of Canada Open-File Report 4350, 17-23.



Wiest, K.R., D.I. Doser, A.A. Velasco, and J. Zollweg, 2007, Source investigation and comparison of the 1939, 1946, 1949 and 1965 earthquakes, Cascadia subduction zone, western Washington, *Pure and Applied Geophysics*, v. 164, p. 1-15.

Youd, T.L., and Idriss, I.M., 1997, Proceedings of the NCEER Workshop on Evaluation of Liquefaction Resistance of Soils, Salt Lake City, UT, January 5-6, 1996, NCEER Technical Report NCEER-97-0022, Buffalo, NY.

Youd, T.L., Hansen, C.M., and Bartlett, S.F., 2002, Revised multilinear regression equations for prediction of lateral spread displacement, *ASCE Journal of Geotechnical and Environmental Engineering*, v. 128, p. 1007-1017.

APPENDIX

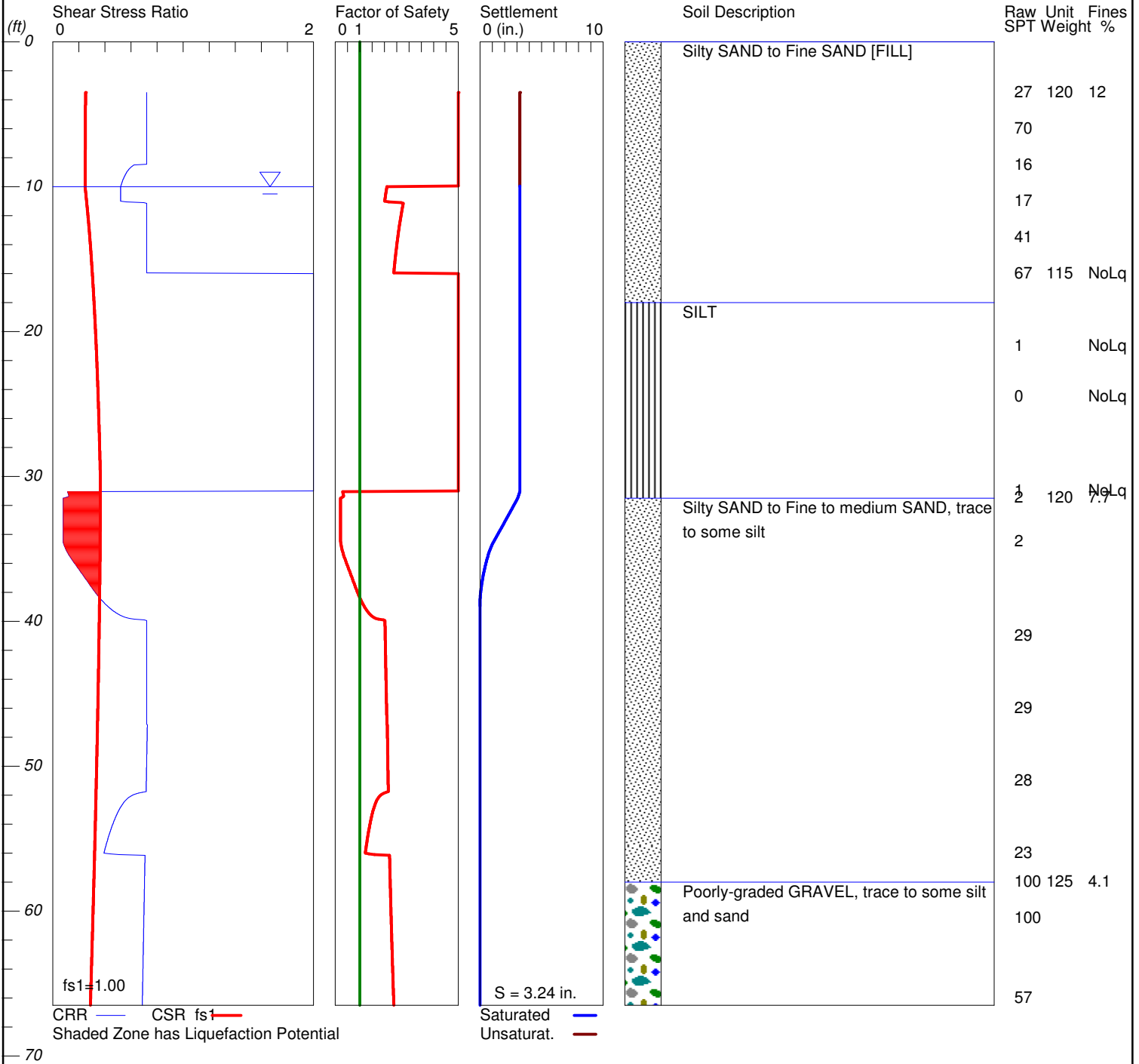
Plots of Liquefaction Potential

LIQUEFACTION ANALYSIS

Tesoro Savage Terminal

Hole No.=B-7 Water Depth=10 ft Surface Elev.=27.9

Magnitude=6.5
Acceleration=0.39g



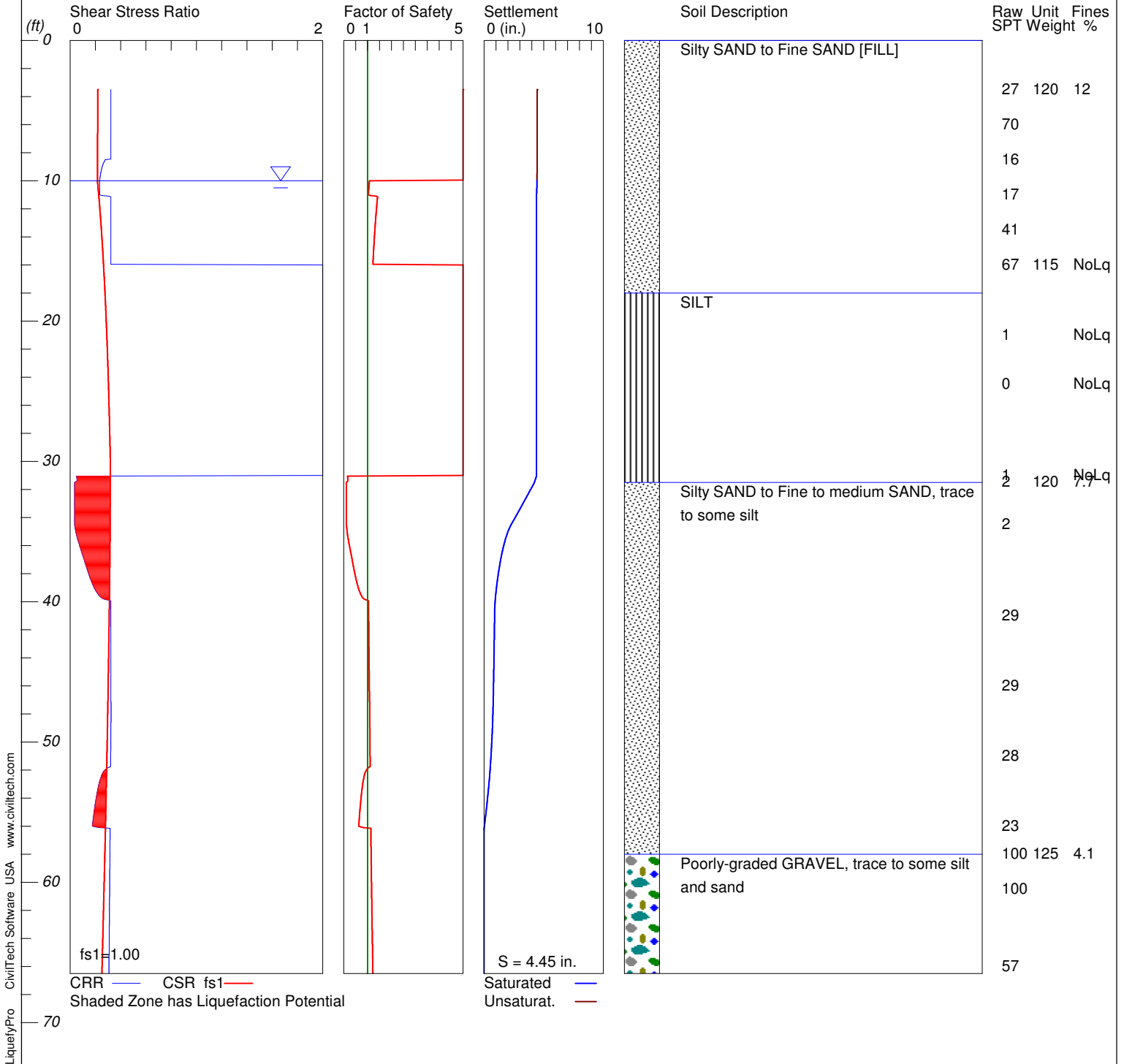
LiquefyPro CivilTech Software USA www.civiltch.com

LIQUEFACTION ANALYSIS

Tesoro Savage Terminal

Hole No.=B-7 Water Depth=10 ft Surface Elev.=27.9

Magnitude=8.9
Acceleration=0.34g

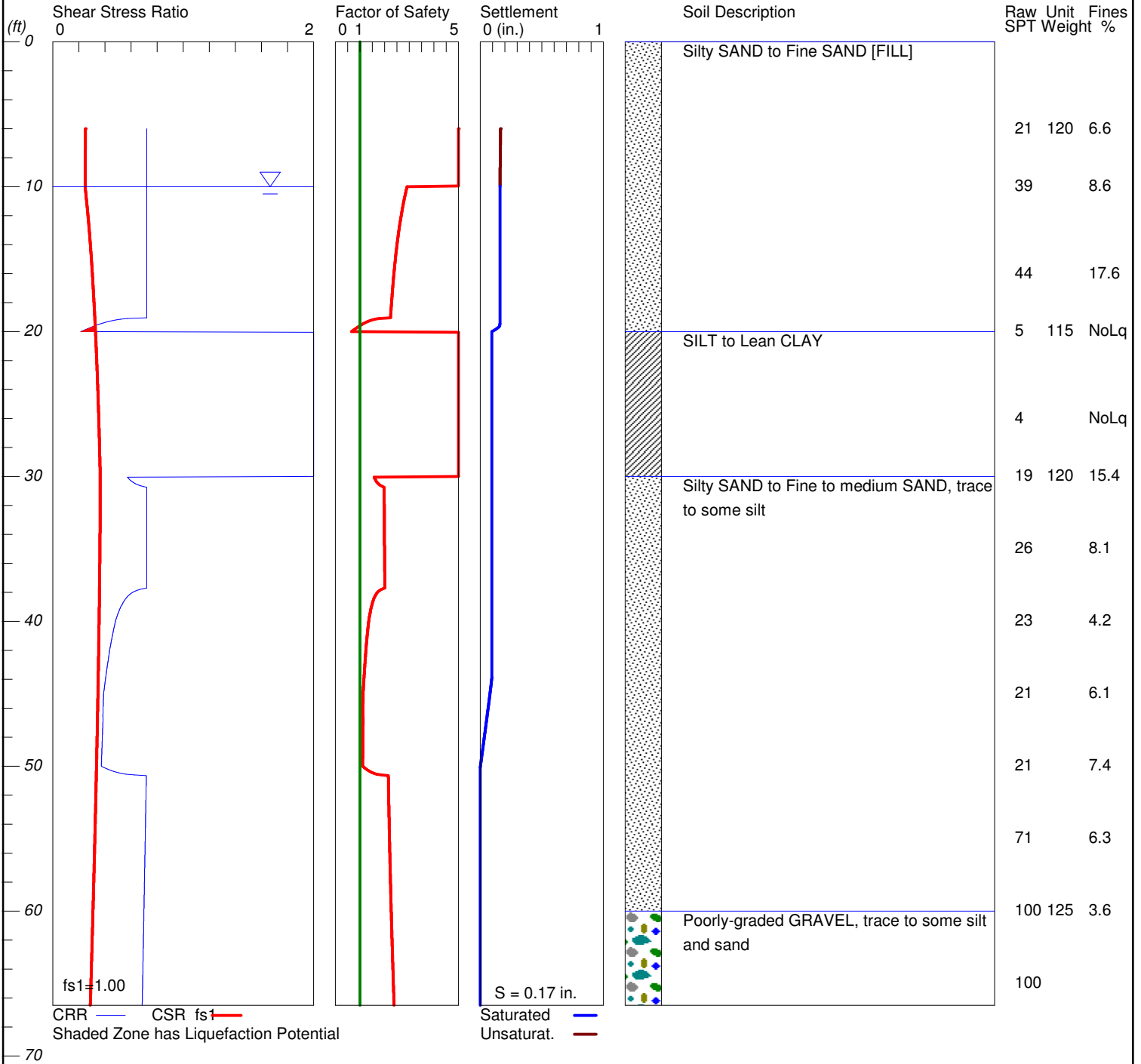


LIQUEFACTION ANALYSIS

Tesoro Savage Terminal

Hole No.=HB-B-108 Water Depth=10 ft Surface Elev.=27.7

Magnitude=6.5
Acceleration=0.39g

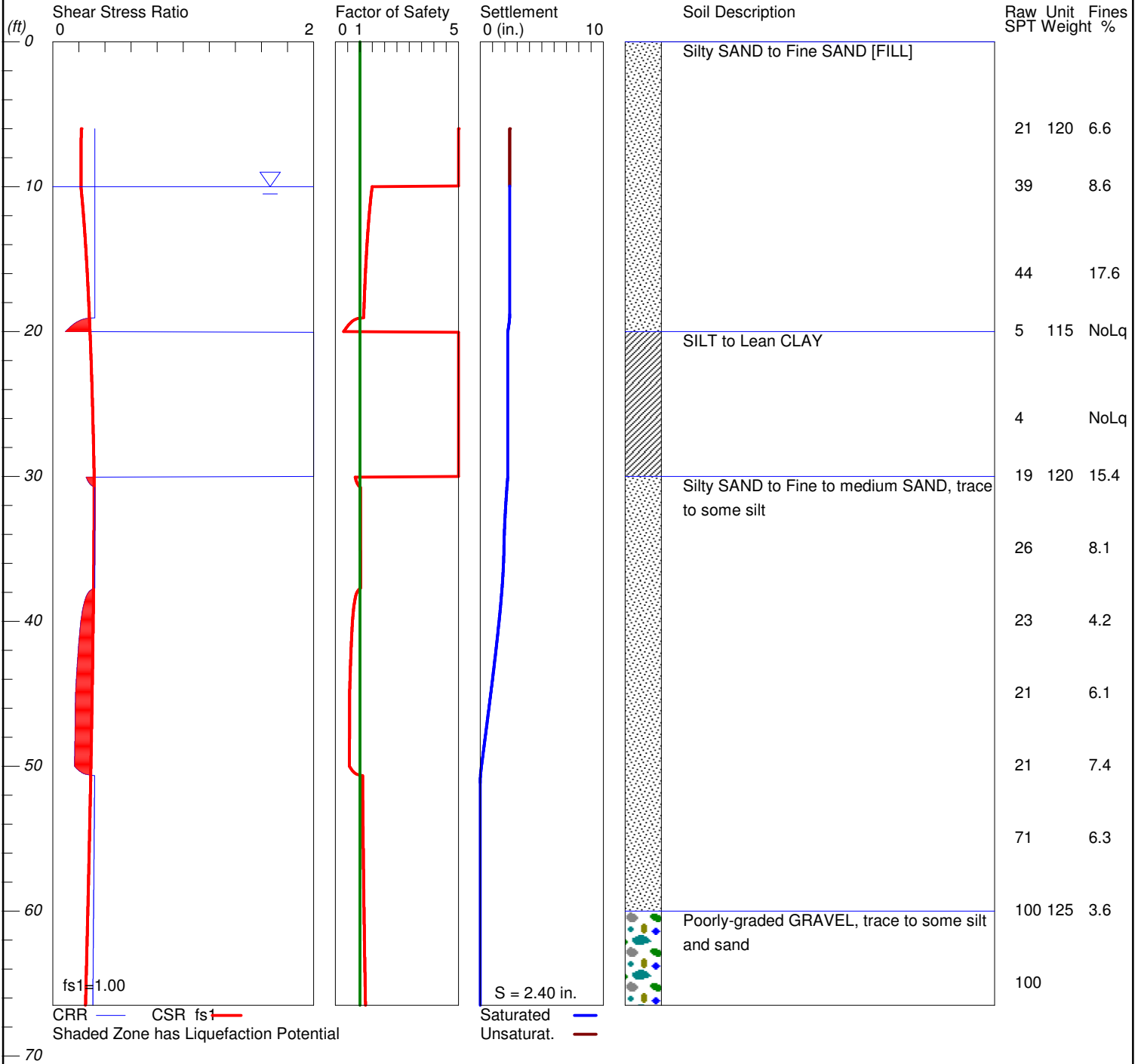


LIQUEFACTION ANALYSIS

Tesoro Savage Terminal

Hole No.=HB-B-108 Water Depth=10 ft Surface Elev.=27.7

Magnitude=8.9
Acceleration=0.34g

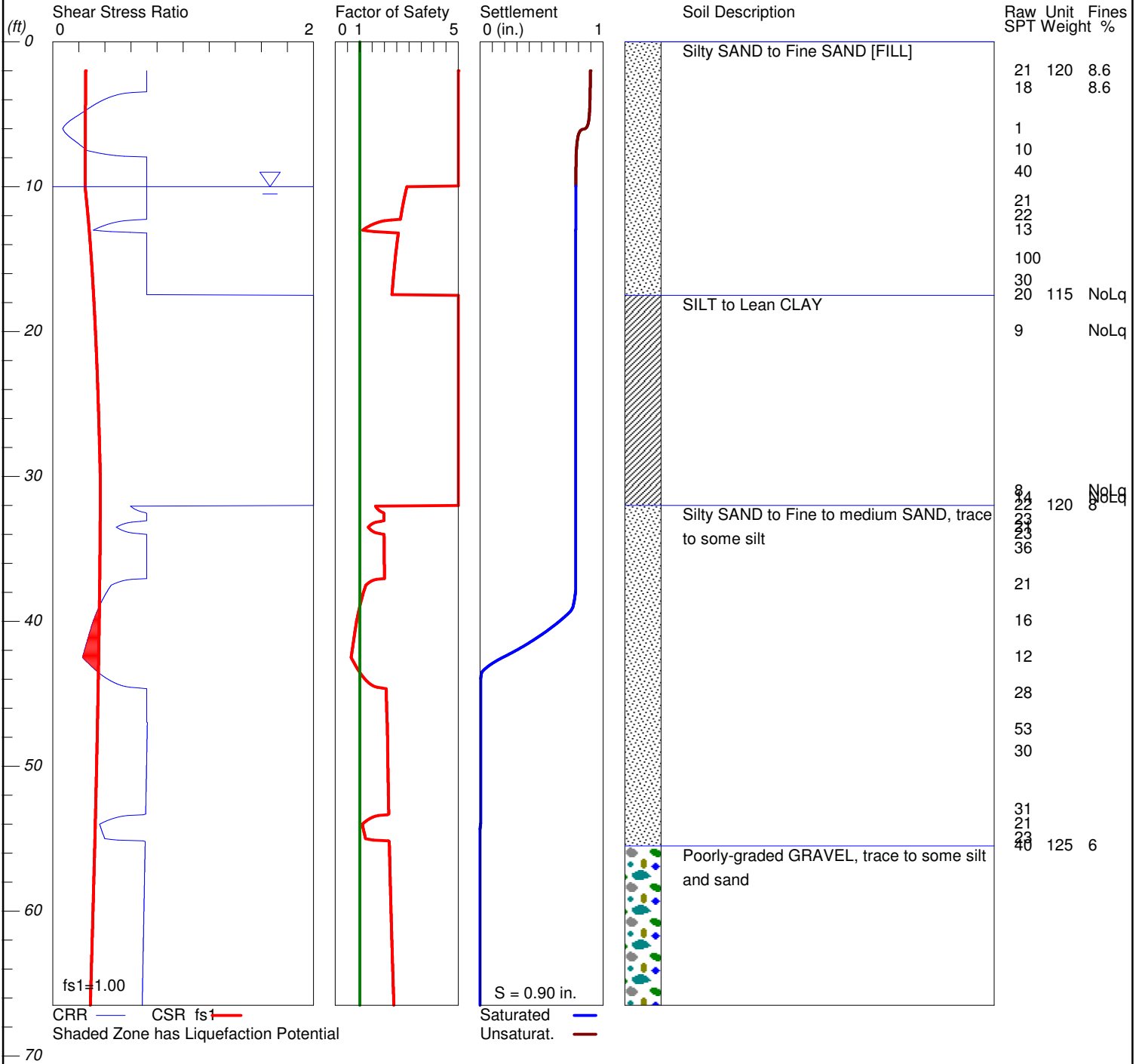


LIQUEFACTION ANALYSIS

Tesoro Savage Terminal

Hole No.=HB-CPT-145 Water Depth=10 ft Surface Elev.=27.8

Magnitude=6.5
Acceleration=0.39g

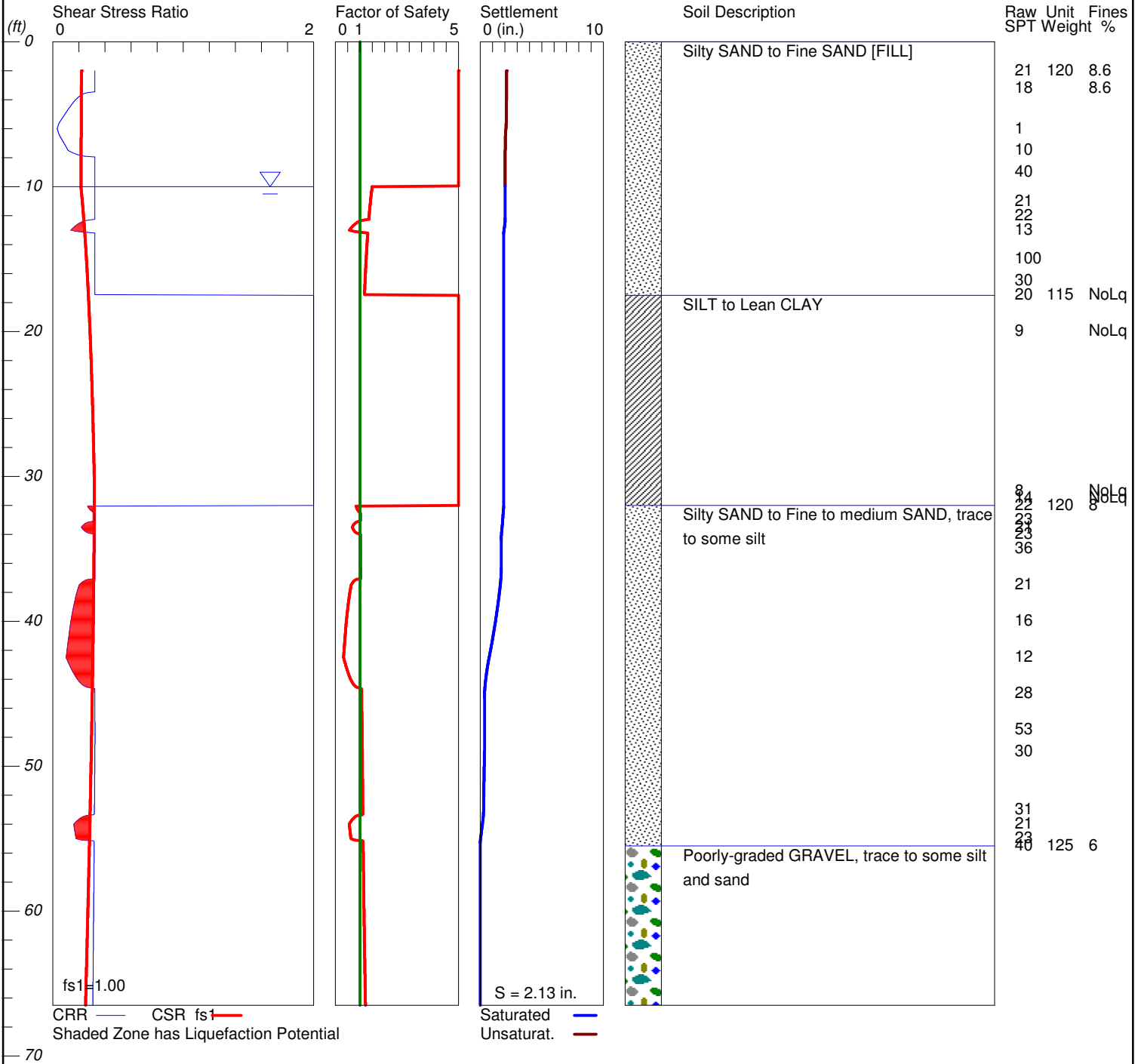


LIQUEFACTION ANALYSIS

Tesoro Savage Terminal

Hole No.=HB-CPT-145 Water Depth=10 ft Surface Elev.=27.8

Magnitude=8.9
Acceleration=0.34g

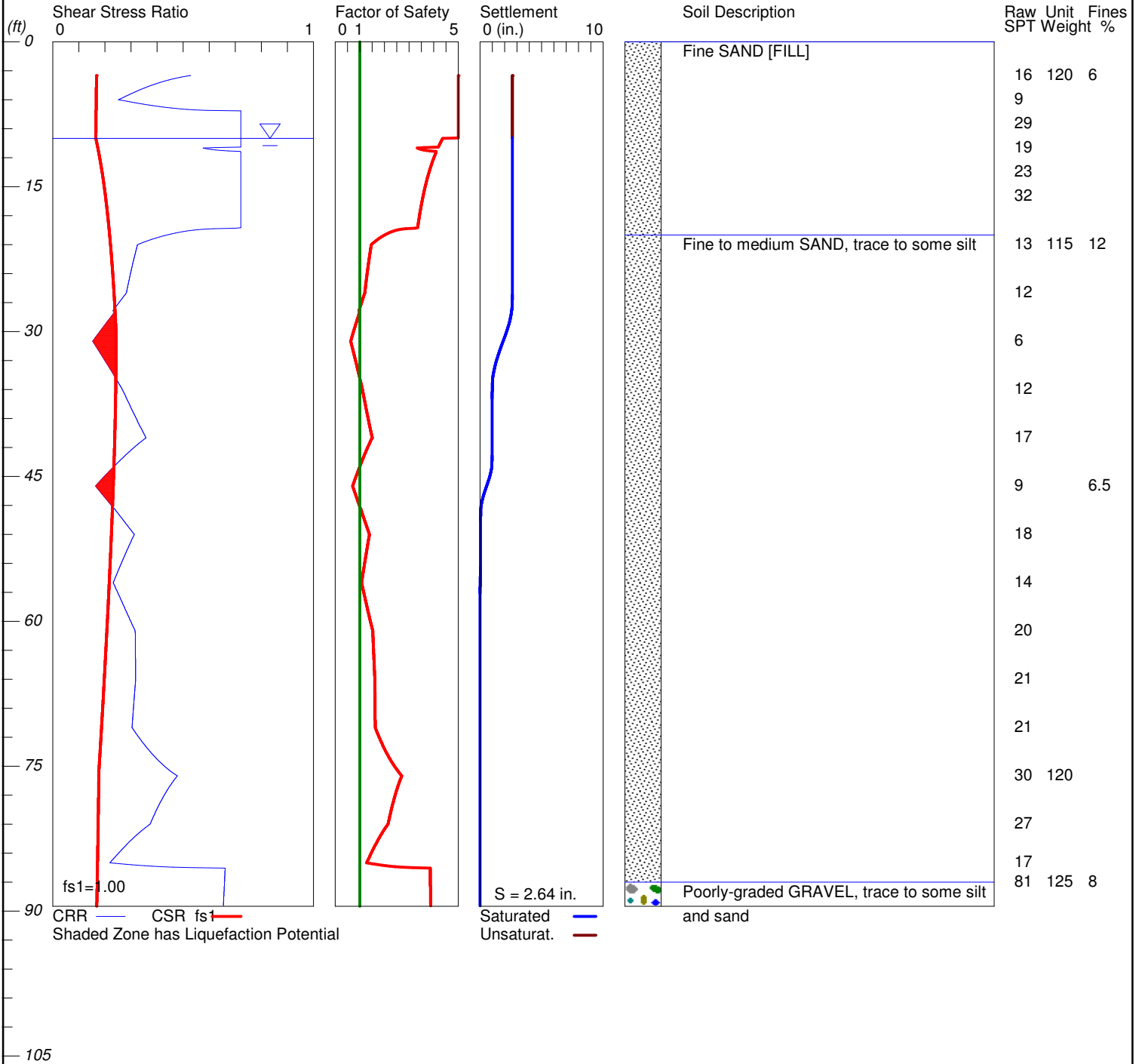


LIQUEFACTION ANALYSIS

Tesoro Savage Terminal

Hole No.=B-23 Water Depth=10 ft Surface Elev.=27

Magnitude=6.5
Acceleration=0.26g



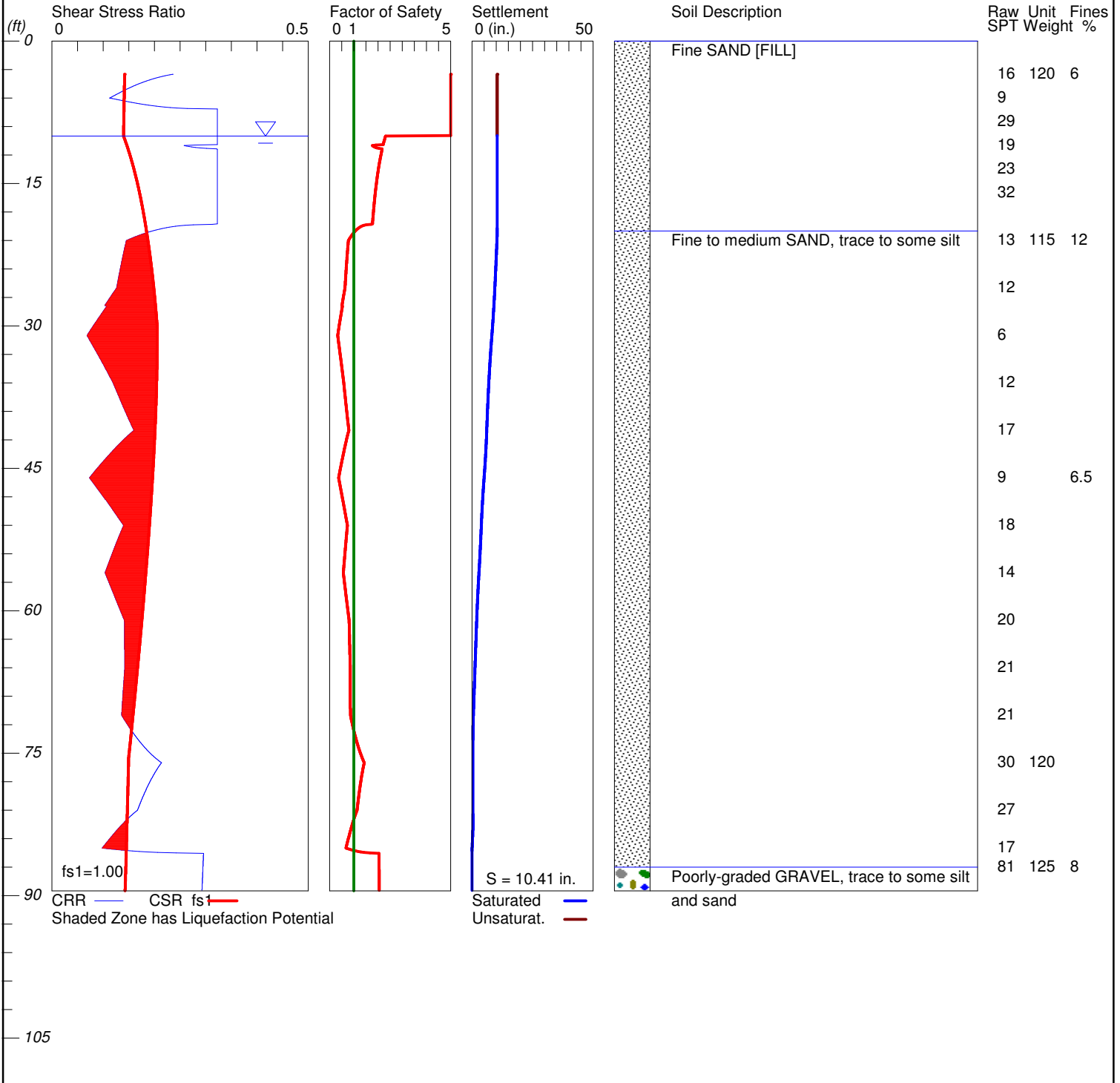
LiquefyPro CivilTech Software USA www.civiltch.com

LIQUEFACTION ANALYSIS

Tesoro Savage Terminal

Hole No.=B-23 Water Depth=10 ft Surface Elev.=27

Magnitude=8.9
Acceleration=0.22g

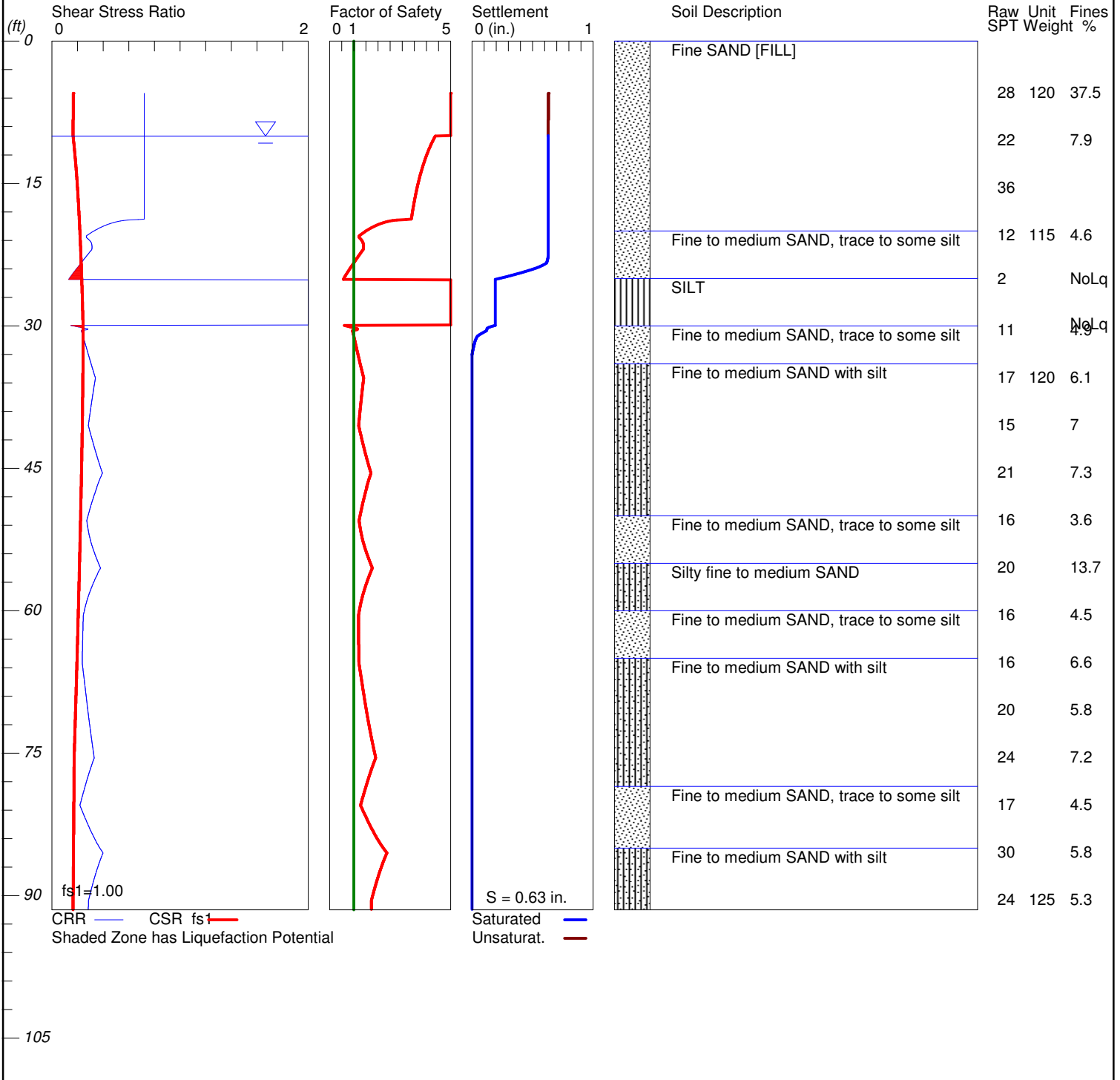


LIQUEFACTION ANALYSIS

Tesoro Savage Terminal

Hole No.=HB-B-109 Water Depth=10 ft Surface Elev.=27.5

Magnitude=6.5
Acceleration=0.26g



LIQUEFACTION ANALYSIS

Tesoro Savage Terminal

Hole No.=HB-B-109 Water Depth=10 ft Surface Elev.=27.5

Magnitude=8.9
Acceleration=0.22g

